Ital. J. Geosci. (Boll. Soc. Geol. It.), Vol. 131, No. 2 (2012), pp. 187-204, 6 figs., 3 tabs. (doi: 10.3301/IJG.2011.31)

Seismic crustal deformation in the Southern Apennines (Italy)

Francesco Visini (*)

ABSTRACT

With the aim of estimating the rates of seismic moment and deformation in seismic zones of southern Italy, constraints on tectonic style and kinematics data from geophysical and geologic data were integrated with the traditional constraints from seismicity catalogues. Seismotectonic considerations indicate that the region can be divided into four broad crustal seismogenic volumes, of relatively homogeneous deformation: an extensional crustal volume in the western part of the Southern Apennines and three crustal volumes characterized by a transcurrent regime in the eastern area.

For each crustal volume, the annual seismic moment release showing the rate of the deformation was estimated by integrating magnitude-frequency relations of historical earthquakes. The application of a Monte Carlo simulation systematically incorporated the uncertainties of the input parameters.

The results show that the westernmost crustal volume is undergoing extension, with velocity of ~1.2 mm/a (along a nearly NE-SW direction), whereas the easternmost volumes are undergoing transcurrent deformation, with an along-strike deformation axis oriented along a nearly E-W direction, with velocities of ~1 mm/a, ~1.2 mm/a and ~0.1 mm/a, respectively for the northern, central and southern volumes.

The errors affecting the estimate of the crustal deformation using the seismicity catalogues may be significant. The parameters with the largest contribution are the coefficients of the magnitude-moment relationship; the second and third contributors are the coefficients of the magnitude-frequency distribution and the maximum magnitude. Uncertainties in the geometrics and kinematics parameters have slight, minor effects. Furthermore, the effects of the crustal model (and the consequent earthquake association) are of the same order as the uncertainties of the parameters involved in the computation.

These results agree with recent GPS data and geological slip rates in terms of direction and rate of deformation.

Key word: *Seismotectonics, crustal deformation, active normal faulting, active strike-slip faulting, Southern Apennines of Italy.*

INTRODUCTION

Knowledge of the velocity and strain tensors of seismogenic deformation and robust estimates of their uncertainties are essential for determining the seismic hazard of an active region, especially in an area with relatively low strain rates. Similarly, the comparison of seismic deformational rates with crustal deformational rates derived from geological and geodetic data has become a major aspect of seismic hazard studies (e.g. Peruzza *et alii*, 2011). Geological data on the long-term deformation history (in the order of 10^4a) may allow us to extend the history of slip of a seismogenic region, to a large number of earthquake cycles (e.g., Papanikolaou *et alii*, 2005; Bull *et alii*, 2006; Nicol *et alii*, 2006). Obviously, the completeness of geological strain rate depends on the availability of quantitative geological data for the study area. Geodetic strain takes into account the total value of the active deformation, but it is unable to discriminate the seismic components from the aseismic ones. Moreover, it is still unclear whether geodetic data, which covers about 10-20 years of measurements, can be extrapolated to longer time periods owing to the short instrumental record (Papanikolaou *et alii*, 2005; Faure Walker *et alii*, 2010).

The seismological approach represents a sort of intermediate approach, with the possibility of covering up to one thousand years. Moreover, the seismological approach remains highly interesting in areas where quantitative geological data are insufficient for detailed slip analysis.

In this paper, a comparison among deformation-rate estimates is presented, including the main uncertainties associated with evaluating the seismic moment, based on different crustal models. The aim is to provide a quantitative evaluation of the influences of the crustal models in terms of geometry, kinematics and consequently of the associated earthquakes on the evaluation of the seismic budget of active crustal deformation.

Southern Italy provides a good testing ground to carry out this comparison. It is one of the most seismically active regions of the central-western Mediterranean area, with earthquakes up to magnitude 7 (fig. 1). After the 1980 Irpinia earthquake, many studies were carried out to investigate the state of stress and the seismotectonic setting of the Southern Apennines. Stress analyses (Montone *et alii*, 2004) and seismologic/seismotectonic studies of the Irpinia, as well as other moderate and minor seismic sequences (Cocco *et alii*, 1999; Frepoli & Amato, 2000; Cucci *et alii*, 2004), indicate prevailing dip-slip kinematics along NW-SE-striking active normal faults, with a sub-horizontal SW-NE-trending extensional direction. This seismicity lies at depths shallower than 15 km within the upper crust (e.g., Westaway & Jackson, 1987; Bernard & Zollo, 1989; Amato & Selvaggi, 1993; Cocco *et alii*, 1999; Chiarabba *et alii*, 2005a; Basili *et alii*, 2008).

However, some moderate-magnitude earthquake sequences do not follow this trend. For instance, the 1990 (M = 5.7) and 1991 (Mw = 5.2) earthquakes in the Potenza area, only 40-50 km ESE of the Irpinia epicentral area, and the 2002 sequence (main event Mw = 5.7) NE of the Southern Apennines show a different pattern of active deformation. In fact, the focal mechanisms of these events (Azzara *et alii*, 1993; Ekstrom, 1994; Di Luccio *et alii*, 2005b; Pon-

(*) Dipartimento di Scienze Umanistiche e della Terra, Università "G. d'Annunzio" di Chieti-Pescara, Campus Universitario, 66013 Chieti Scalo, Italia, tel. 0039 0871 355 6518; fax 0039 0871 355 6454; f.visini@unich.it

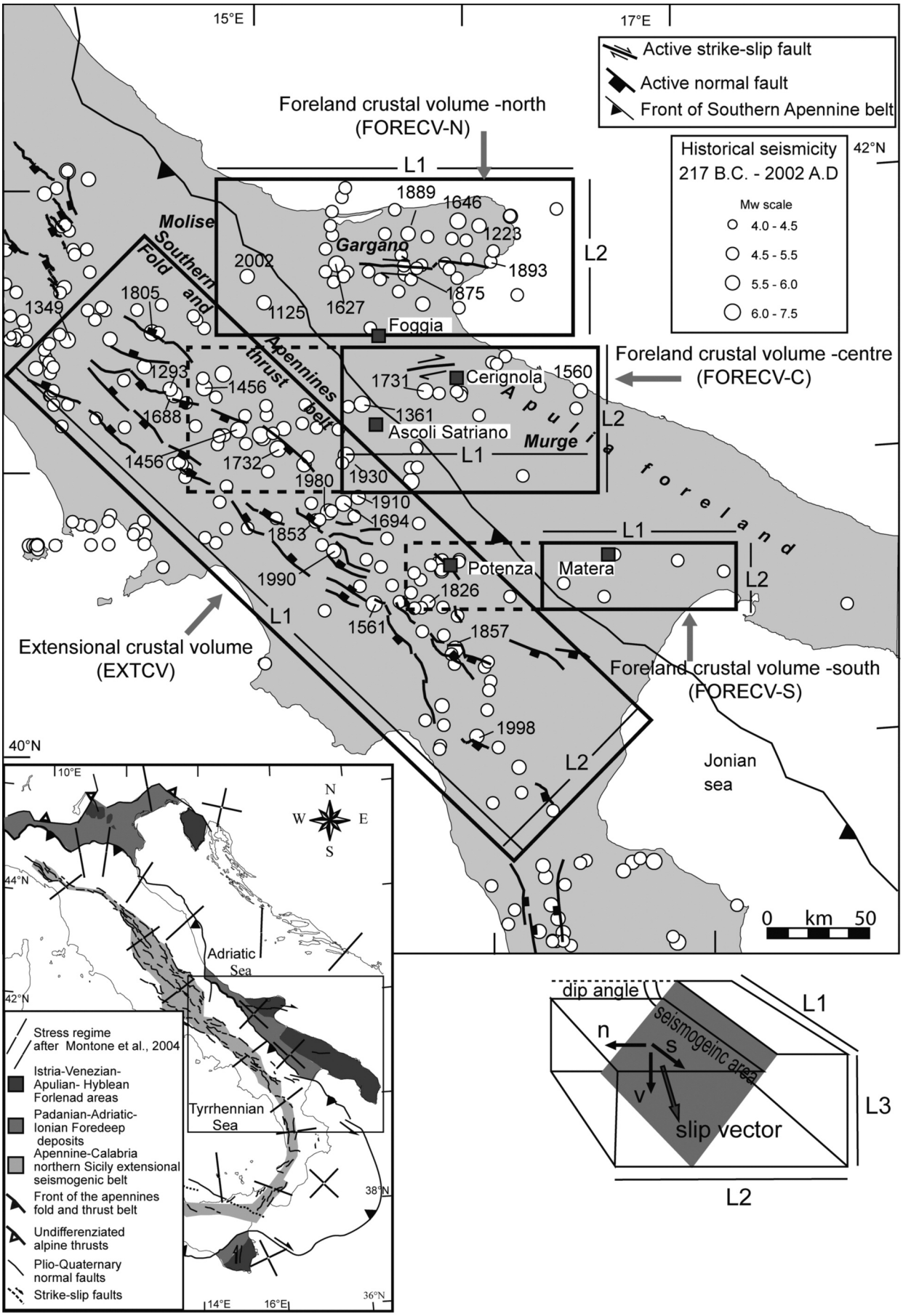
15°E
17°E
42°N
40°N
Active strike-slip fault
Active normal fault
Front of Southern Apennine belt
Historical seismicity
217 B.C. - 2002 A.D
Mw scale
4.0 - 4.5
4.5 - 5.5
5.5 - 6.0
6.0 - 7.5
Foreland crustal volume -north
(FORECV-N)
Foreland crustal volume -centre
(FORECV-C)
Foreland crustal volume -south
(FORECV-S)
Extensional crustal volume
(EXTCV)
L1
L2
L3
Molise
Gargano
Southern Fold and thrust Apennines belt
Apulia foreland
Murge
Foggia
Cerignola
Ascoli Satriano
Potenza
Matera
Jonian sea
1889
1646
1223
1893
1875
1627
1125
2002
1805
1349
1293
1456
1688
1456
1732
1980
1930
1910
1694
1853
1990
1826
1561
1857
1998
1731
1361
1560
0 km 50
10°E
44°N
42°N
38°N
36°N
14°E
16°E
N
S
W
E
Adriatic Sea
Tyrrhennian Sea
Stress regime after Montone et al., 2004
Istria-Venezian-Apulian- Hyblean Forlenad areas
Padanian-Adriatic-Ionian Foredeep deposits
Apennine-Calabria northern Sicily extensional seismogenic belt
Front of the apennines fold and thrust belt
Undifferenziated alpine thrusts
Plio-Quaternary normal faults
Strike-slip faults
dip angle
seismogeinc area
n
s
v
slip vector

Fig. 1.

DRELLI *et alii*, 2006; BONCIO *et alii*, 2007) indicate nearly pure strike-slip kinematics on E-W trending structures, significantly different from the Apennines extensional seismicity. The focal depths (between 15 and 25 km for the 1990-1991 seismic sequences and 10 to 25 km for the 2002 sequence) also provided evidence that in this part of the chain, toward the foreland of the former fold and thrust belt, NW-SE normal faulting gives way to E-W, right-lateral seismogenic faults (e.g., DI LUCCIO *et alii*, 2005a; VALLÉE & DI LUCCIO, 2005; DI BUCCI *et alii*, 2007; DI BUCCI *et alii*, 2010; FREPOLI *et alii*, 2011).

Obviously, only the seismic part of the strain rate tensor is estimated from seismicity data. Its estimation depends strongly on the completeness of the seismicity catalogue. Although focal mechanisms and precise magnitudes have been available since 1970-1980, this time interval is too short to cover the recurrence time of most of the large earthquakes (e.g., VALENSISE & PANTOSTI, 2001). It is likely that the amplitude of seismic deformation based on instrumental seismicity is significantly lower than the real amplitude. Therefore, in this paper, the rates of deformation are evaluated using both instrumental and historical catalogues.

Bearing in mind the potential pitfalls of the common analysis of seismological data and of the consequences in the determination of active crustal deformation (e.g., values of magnitude and estimation of Gutenberg-Richter parameters), an analysis of these errors is also performed following the Monte Carlo method proposed by PAPAZACHOS & KIRATZI (1992).

METHODOLOGY AND INPUT DATA

In order to estimate the seismic deformation in the Southern Apennines of Italy, seismic catalogues analyses, geophysical data and geological information were integrated.

Starting from the assumptions that the deformation of a region is represented by a characteristic tectonic style and that the magnitude-frequency distribution of earthquakes applies uniformly to the entire crustal volume, the relation between the seismic moment rate $\dot{M}o$ and the amount of slip rate s is expressed as:

$$\dot{M}o = \mu s A \tag{1}$$

where μ is the rigidity of crustal rocks, and A is the fault rupture area. From equation (1) the vertical (v), normal (n), and along-strike (s) components of the relative block motion, as illustrated in the inset of fig. 1, are:

$$v = (\sin(rake)\sin^2(dip)\dot{M}o)/\mu L1L3 \tag{2}$$

$$n = (\sin(rake)\cos(dip)\sin(dip)\dot{M}o)/\mu L1L3 \tag{3}$$

$$s = (\cos(rake)\sin(dip)\dot{M}o)/\mu L1L3 \tag{4}$$

where L1 and L3 are the length and seismogenic thickness of the crustal volume, respectively, and $\dot{M}o$ is the rate of seismic moment release as estimated from earthquakes that occurred within the crustal volume in the years of the completeness interval.

The scalar seismic moment rate ($\dot{M}o$) can be calculated using MOLNAR's (1979) formula:

$$\dot{M}o = \frac{A}{1-B} Mo_{\max}^{1-B} \tag{5}$$

with:

$$Mo_{\max} = 10^{cM\max+d} \tag{6}$$

$$A = 10^{[a+(bd/c)]} \tag{7}$$

$$B = \frac{b}{c} \tag{8}$$

The parameters a and b are values of the Gutenberg-Richter (GUTENBERG & RICHTER, 1944) relation (values and uncertainties calculated in this paper, see paragraph 2.4), c and d are constants of the moment-magnitude relation (1.5 and 9.1, KANAMORI & ANDERSON, 1975), and $Mo_{\max}$ is the scalar moment of the largest observed earthquake in the region. The advantage of this formula is that the full record of seismicity in any given region can be used.

The input data to calculate the seismic budget of active crustal deformation can be summarized as follows:

(i) Dimensions of the crustal seismogenic volumes, deduced from integrated geological-seismological constraints (paragraph 2.1);

(ii) Kinematics of the crustal seismogenic volumes, computed from reliable fault plane solutions (paragraph 2.2);

(iii) Earthquake dataset for each crustal volume (paragraph 2.3);

(iv) Magnitude-frequency distributions that will be used to calculate the seismic moment rates (paragraph 2.4).

DIMENSIONS OF THE CRUSTAL SEISMOGENIC VOLUMES

To take into account a kinematics setting characterised by extension in the axial zone of the Southern Apennines and transcurrent in the Apulia foreland, I assumed 4 broad crustal volumes undergoing active deformation, one NW-SE oriented (EXTCV in figs. 1 and 2) in which the extensional seismogenic sources are comprised, and three E-W oriented crustal volumes (FORECV-N, FORECV-C and FORECV-S in figs. 1 and 2) undergoing strike-slip tectonics and located in the foreland. Moreover, owing to the overlapping of the tectonic regimes documented in a part of the Southern Apennines chain, two main geometric models of crustal volumes were used. In the first any overlapping was avoided for the two volumes using a 2D plan view to extract earthquakes falling inside each crustal volume (hereinafter named "model A":

Fig. 1 - Seismotectonic sketch of the Southern Apennines with locations of major active faults and historical seismicity. Major faults are from PANTOSTI & VALENSISE (1990); CINTI *et alii* (1997); MENARDI NOGUERA & REA (2000); MASCHIO *et alii* (2005); and BONCIO *et alii* (2007). Historical seismicity is from WORKING GROUP CPTI (2004). The region is divided into four broad crustal volumes (solid and dashed black lines show the dimensions of the crustal volumes used in this work). L1, L2 and L3 are the dimensions of the sources as reported in tab. 2. The left-lower inset shows the location of fig. 1 within the seismotectonics and the stress field of the Italian territory. The right-lower inset shows the relation between deformation of a seismic zone and characteristic fault parameters: slip vector, dip, and rake of slip along the fault; n, s, and v, are the normal, along-strike, and vertical components, respectively, of relative block motion across the seismic zone associated with slip on the fault.

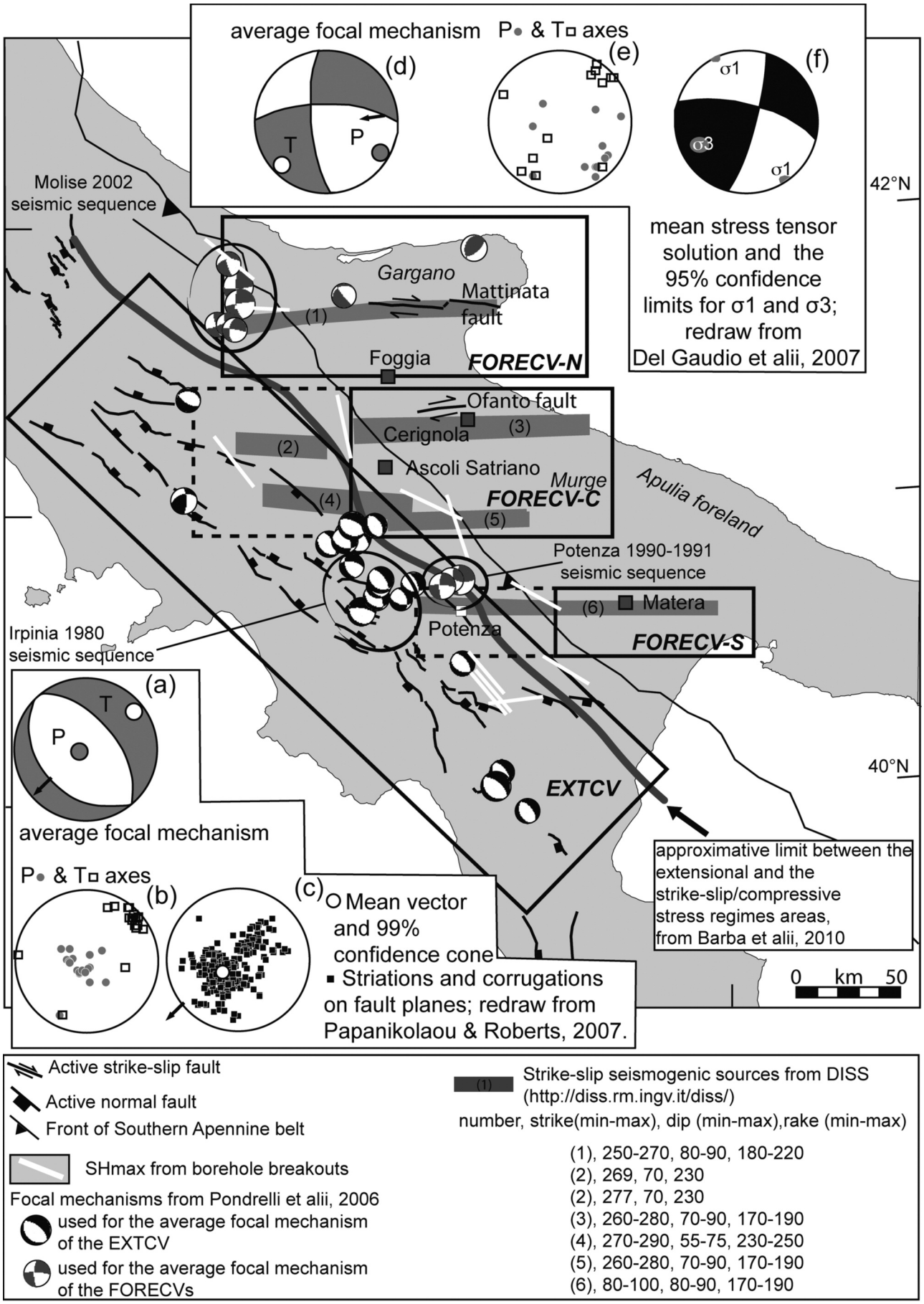
average focal mechanism
P• & T□ axes
(d)
(e)
(f)
T
P
σ1
σ3
σ1
mean stress tensor solution and the 95% confidence limits for σ1 and σ3; redraw from Del Gaudio et alii, 2007
42°N
Molise 2002 seismic sequence
Gargano
Mattinata fault
(1)
Foggia
FORECV-N
Ofanto fault
Cerignola
(3)
(2)
Ascoli Satriano
Murge
FORECV-C
(4)
(5)
Apulia foreland
Potenza 1990-1991 seismic sequence
(6)
Matera
Potenza
FORECV-S
Irpinia 1980 seismic sequence
(a)
T
P
average focal mechanism
P• & T□ axes
(b)
(c)
Mean vector and 99% confidence cone
Striations and corrugations on fault planes; redraw from Papanikolaou & Roberts, 2007.
40°N
EXTCV
approximative limit between the extensional and the strike-slip/compressive stress regimes areas, from Barba et alii, 2010
0 km 50
Active strike-slip fault
Active normal fault
Front of Southern Apennine belt
SHmax from borehole breakouts
Focal mechanisms from Pondrelli et alii, 2006
used for the average focal mechanism of the EXTCV
used for the average focal mechanism of the FORECVs
(1)
Strike-slip seismogenic sources from DISS (http://diss.rm.ingv.it/diss/)
number, strike(min-max), dip (min-max),rake (min-max)
(1), 250-270, 80-90, 180-220
(2), 269, 70, 230
(2), 277, 70, 230
(3), 260-280, 70-90, 170-190
(4), 270-290, 55-75, 230-250
(5), 260-280, 70-90, 170-190
(6), 80-100, 80-90, 170-190

Fig. 2.

solid black rectangles in figs. 1 and 2); for the second model a simplified 3D view was used, with overlapping volumes (hereinafter named "model B": solid + dashed black rectangles in figs. 1 and 2). To parameterise the dimensions (length L1, width L2, thickness L3) of each deforming seismogenic crustal volume, investigation was carried on the current tectonic style, integrating geologic data with the traditional constraints from instrumental seismicity catalogues and with other geophysical data.

Extensional Crustal Volume (EXTCV)

As shown in figs. 1 and 2, many active faults are defined in the area of largest seismicity that is mostly concentrated in a narrow belt along the axis of the Apennines (e.g. PANTOSTI *et alii*, 1993; BENEDETTI *et alii*, 1998; CELLO *et alii*, 2003; MASCHIO *et alii*, 2005; BASILI *et alii*, 2008; FREPOLI *et alii*, 2011). Generally, the seismicity of the last 30 years (CASTELLO *et alii*, 2005; FREPOLI *et alii*, 2011) shows hypocentral depths shallower than 15-20 km. The present day orientation of the active normal faults in the Apennines is mostly strike parallel to the mountain chain (ANDERSON & JACKSON, 1987; CINQUE *et alii*, 2000; BROZZETTI, 2011), with an average direction of extension about NE-SW oriented (e.g. PAPANIKOLAOU & ROBERTS, 2007), consistent with borehole break-out data and focal mechanisms (e.g. MONTONE *et alii*, 2004; PONDRELLI *et alii*, 2006; BARBA *et alii*, 2010).

Information on paleoseismicity and deformation rates can be also derived from paleoseismological investigations, for example on the Irpinia fault (WESTAWAY & JACKSON, 1987; BERNARD & ZOLLO, 1989; PANTOSTI & VALENSISE, 1990; PORFIDO *et alii*, 2002). Trenching of the fault responsible for the 1980 earthquake supplied evidence for at least four of its predecessors occurring every 2000 years on average (PANTOSTI *et alii*, 1993). Subsequent trenching of a number of large faults, confirmed these findings and returned fundamental constraints on the frequency of large Apennines earthquakes (see VALENSISE & PANTOSTI, 2001 and GALLI *et alii*, 2008 for a review).

To take into account the pattern of major faults mapped in the area, the spatial concentration of the seismic events (fig. 1), normal fault plane solutions and borehole break-out data (fig. 2), here I used an extensional crustal volume with an along-strike extent (L1) of 275 km, a width (L2) of 75 km and a seismogenic thickness (L3) of 15 km (EXTCV in tab. 2).

Foreland Crustal Volumes

Drawing from recent focal mechanism solutions (e.g. PONDRELLI *et alii*, 2006; DEL GAUDIO *et alii*, 2007; FREPOLI *et alii*, 2011), geodetic data (e.g. SERPELLONI *et alii*, 2005; FERRANTI *et alii*, 2008) and numerical simulation (e.g. BARBA *et alii*, 2010), the extensional crustal volume in the western part of the Southern Apennines was separated from a transcurrent regime in the eastern area. Three crustal volumes located in the north, central and south of the Apulia foreland were described.

TABLE 1

Hypocentral and fault plane parameters of the events with Mw≥4.0 occurring since 1977. Data from PONDRELLI *et alii* (2006).

Longitude	Latitude	depth	strike	dip	rake	Mw	month	day	year
16.21	39.3	15	14	43	-78	4.4	2	20	1980
16.12	39.94	15	157	35	-80	4.7	3	9	1980
15.85	40.46	18.4	119	38	-112	4.8	5	14	1980
15.37	40.91	13.7	135	41	-80	6.9	11	23	1980
15.26	40.89	20.2	131	29	-110	5	11	24	1980
15.33	40.9	15	115	44	-125	5	11	24	1980
15.4	40.65	15	129	26	-65	5.4	11	25	1980
15.47	40.7	18.9	122	30	-119	4.9	11	25	1980
15.48	40.74	19.3	148	36	-76	4.8	12	3	1980
15.37	40.95	15	115	30	-93	5.2	1	16	1981
14.6	41.05	15	254	46	157	4.9	2	14	1981
15.64	40.74	15	104	41	-138	4.5	11	29	1981
15.36	40.81	17.8	158	48	-45	4.7	8	15	1982
15.47	40.95	15	160	45	-79	4.5	1	28	1987
16.01	40.08	16.4	148	30	-86	4.7	1	8	1988
15.85	40.75	26	184	73	-13	5.8	5	5	1990
15.81	40.75	15	282	83	-173	4.8	5	5	1990
15.77	40.73	20	183	71	-9	5.1	5	26	1991
14.3	42.43	15	89	29	-138	4.2	7	16	1992
15.97	41.9	24	197	32	58	5.2	9	30	1995
15.49	40.76	21.5	123	30	-110	4.9	4	3	1996
14.63	41.4	10	280	27	-110	4.5	3	19	1997
15.98	40.03	15	139	29	-83	5.6	9	9	1998
15.36	41.75	10	246	19	-166	4.5	7	2	2001
15.58	40.69	15	340	49	-52	4.4	4	18	2002
14.87	41.79	15	180	79	11	5.7	10	31	2002
14.88	41.73	15	171	66	-5	5.7	11	1	2002
14.83	41.87	26	263	56	-166	4.5	11	1	2002
14.77	41.66	20.9	72	80	171	4.6	11	12	2002
14.82	41.66	18.8	167	72	-12	4.5	6	1	2003
14.85	41.64	15.6	187	53	-6	4.5	12	30	2003

Foreland Crustal Volume North (FORECV-N)

According to CASTELLO *et alii* (2005) and to the recent analysis of background seismicity performed by FREPOLI *et alii* (2011), the hypocentral distribution of instrumental earthquakes shows a seismogenic thickness of about 20 km beneath the Apulia forelands. Furthermore, a detailed analysis of the instrumental seismicity located in the Gargano, carried out by DEL GAUDIO *et alii* (2007), showed some distinct clusters, mainly corresponding to a

Fig. 2 - Map of Southern Apennines with locations of major active faults, focal mechanisms, borehole breakouts and seismogenic sources. Focal mechanisms of major instrumental earthquakes (Mw>4.0) that occurred in the time interval 1977-2006 (black focal mechanisms associated with extensional tectonics regime; grey focal mechanisms associated with strike-slip tectonic regime) are from PONDRELLI *et alii* (2006). SHmax orientations are from BARBA *et alii* (2010). KEY: (*a*) and (*d*) average focal mechanisms; (*b*) lower hemisphere stereographic projections of P and T axes of the black focal mechanisms mapped in the main frame of the figure; (*c*) lower hemisphere stereographic projections of striations and corrugations on fault planes from the centres of the faults in southern Italy, with the mean vector and 99% confidence cone, redrawn from PAPANIKOLAOU & ROBERTS (2007); (*e*) lower hemisphere stereographic projections of P and T axes of the grey focal mechanisms mapped in the main frame of the figure; (*f*) stress inversion results using all the focal mechanisms resolved in the Apulia region, redrawn from DEL GAUDIO *et alii* (2007), with the 95% confidence limits for $\sigma 1$ and $\sigma 3$.

TABLE 2

Model parameters used for the calculation and obtained velocity tensors for the different dimensions and GR values as discussed in the text. KEY: L1 = length along strike of the crustal volume; L2 = length normal to strike; L3 = thickness of the seismogenic layer; a and b = GR coefficients; $\dot{M}_o$ = seismic moment rate; n, s, and v = normal, along-strike, and vertical component of relative block motion across the seismic zone.

	GEOMETRIC CONSTRAINTS			RESULTS					
	L1(km)	L2(km)	L3(km)	a±std	b±std	Component of the velocity vector	Value (mm/a)	± std (mm/a)	$\dot{M}o$ ± std e+16(Nma^{-1})
Extensional Crustal Volume Model A	275	75	15	4.23±0.17	-0.97±0.03	n	1.21	0.55	30.39 ± 13.53
						v	1.45	0.67	
						s	0.00	0.18	
Extensional Crustal Volume Model B	275	75	15	4.26±0.18	-0.98±0.03	n	1.12	0.51	28.04 ± 12.51
						v	1.34	0.62	
						s	0.00	0.16	
* Foreland Crustal Volume - north Model A	170	44	15	4.09±0.42	-1.03±0.08	n	0.11	0.07	8.23 ± 4.51
						v	0.33	0.20	
						s	0.96	0.54	
Foreland Crustal Volume - centre Model A	110	44	15	2.53±0.29	-0.79±0.06	n	0.07	0.04	3.12 ± 1.49
						v	0.19	0.11	
						s	0.56	0.28	
Foreland Crustal Volume - centre Model B	190	44	15	2.14±0.20	-0.71±0.04	n	0.14	0.09	11.76 ± 6.01
						v	0.42	0.25	
						s	1.23	0.64	
Foreland Crustal Volume - south Model A	98	19	15	3.06±0.3	-1.00±0.1 (fixed)	n	0.00	0.00	0.16 ± 0.07
						v	0.01	0.00	
						s	0.03	0.01	
Foreland Crustal Volume - south Model B	150	19	15	2.90±0.52	-0.91±0.10	n	0.01	0.01	0.80 ± 0.41
						v	0.03	0.02	
						s	0.11	0.05	

* I did not define a model B for this crustal volume.

few seismic sequences, with focal depths between 5 and 15 km. MILANO *et alii* (2005) showed that the Gargano seismicity is generated by E-W, right-lateral strike-slip faults and by NW-SE, normal to left-lateral second-order faults slipping in response to dominantly NW-SE shortening. The 31 October to 1 November 2002 Molise earthquake sequence, composed of two similarly large (Mw 5.8-5.7) and relatively deep (16-18 km) main shocks, showed the same pure right-lateral focal mechanism on E-W nodal planes (VALLÉE & DI LUCCIO, 2005).

The Mattinata Fault is the most important fault and the only one outcropping of the E-W fault system cutting the northern foreland sector (DI BUCCI *et alii*, 2010). Mesostructural data, mainly from faults cutting Mesozoic limestones, show that the strongest structural imprint at the mesoscale is given by the left-lateral strike-slip kinematics, accompanied by secondary faults, a pull-apart basin and closely spaced dissolution-related cleavage (BILLI, 2003). Field evidence, however, shows that the slip switched to right-lateral around the beginning of the Middle Pleistocene (PICCARDI, 1998, 2005; TONDI *et alii*, 2005). The possible continuation of this shear zone further to the west was first hypothesized by FINETTI (1982) and definitively confirmed by the 2002 Molise earthquakes (see DI BUCCI *et alii*, 2010 for a detailed seismotectonic analysis of the onshore and offshore Gargano fault system).

Moreover, the Database of Italian Seismogenic Sources (version 3.1.1, http://diss.rm.ingv.it/diss/) depicted an E-W trending seismogenic sources, showing a right-lateral kinematics, involving the full length of the Gargano Promontory (fig. 2).

Considering the epicentral distribution of the historical seismicity, the hypocentral distribution of instrumental seismicity and the geological data, here I used an E-W orientated transcurrent crustal volume with an along-strike extent (L1) of 170 km, a width (L2) of 44 km and a seismogenic thickness (L3) of 15 km (FOREV-N in tab. 2).

Foreland Crustal Volume Central (FORECV-C) and Foreland Crustal Volume South (FORECV-S)

Recently, for the central and southern part of the Apulia foreland, FREPOLI *et alii* (2011) highlighted the fact that the recent seismic activity is also present in the Matera

and Cerignola areas, with the focal mechanisms available for these sectors showing a NNW-SSE P-axis orientation.

Moreover, within the extensional area of the Apennines at least two seismic clusters, showing an E-W elongation, were recognised by FREPOLI *et alii* (2011). One is located in the same area as the two Potentino sequences of 1990 and 1991 and shows hypocentral depths between 15 and 25 km. Directly to the south, the second cluster extends from the ~10 km south of Potenza to ~15 km south-west of Matera, with focal depths between 15 and 40 km. According to BONCIO *et alii* (2007) and to FREPOLI *et alii* (2011), this pattern suggests the presence of an overlap between the inner portion of the chain, characterized by extension, and the foreland area, where dextral strike-slip kinematics prevail.

Finally, the Database of Italian Seismogenic Sources (version 3.1.1, http://diss.rm.ingv.it/diss/) indicated five seismogenic sources, about E-W oriented, showing a right-lateral kinematics and a seismogenic depths ranging from 5 to 20 km, matching the shape of the two broad crustal volumes identified in this sector of the Apennines (fig. 2). Considering this complex seismotectonic setting, for two crustal volumes undergoing strike-slip kinematics (FORECV-C and FORECV-S), a possible extension beneath the extensional area has been tested (dashed rectangles in fig. 2, model B). The dimensions of FORECV-C are: L1 = 110 km (L1 = 190 km for the model B), L2 = 44 km, L3 = 15 km; the dimensions of FORECV-S are L1 = 98 km (150 km for the model B), L2 = 19 km and L3 = 15 km (tab. 2).

KINEMATICS

Because the kinematics of each crustal volume is given in terms of rake and dip (eqs. 2-4), I computed an average focal mechanism through the application of a Linked Bingham Distribution (ALLMENDINGER, 2001) procedure, which is the equivalent of an unweighted moment tensor summation. All focal mechanisms available in the literature were selected for the events with moment magnitudes Mw>4.0 that occurred in the time interval 1977-2006 within the four crustal volumes (fig. 2; tab. 1, dataset from PONDRELLI *et alii*, 2006). An average focal mechanism for the EXTCV was computed together with a second focal mechanism common to FORECV-N, FORECV-C and FORECV-S.

In the EXTCV, prevailing normal to normal/oblique kinematics characterise the 1980 seismic sequence and many other events. In fig. 2, the focal solutions used to compute the average focal mechanisms are identified by black quadrants. The computed average focal mechanism is shown in fig. 2a.

In the FORECV-N, FORECV-C and FORECV-S, prevailing strike-slip solutions are typical of the 2002 and 1990-1991 sequences and of the remaining selected events. In fig. 2, the events used to compute the average focal mechanism shown in fig. 2d, are identified by grey quadrants.

The main consequence of such a procedure is the assumption of recent kinematics for historical earthquakes by means of recent focal mechanisms. This choice, however, is certainly corroborated by the matching between the recent deformation axes of focal solutions and slip vectors measured on fault planes (fig. 2).

In the extensional area of the southern Apennines, PAPANIKOLAOU & ROBERTS (2007) collected a huge database of slip vectors on the main active faults of the Southern Apennines and calculated the mean fault slip direction and hence the kinematics for the active fault array. Their calculated mean fault slip direction for the active fault array is ~70° plunging towards ~230°. This is consistent with the NE-SW σ3 orientation of the active stress field (MONTONE *et alii*, 2004) and with the T axis of the average focal mechanism computed in this work (fig. 2). Moreover, the direction computed by PAPANIKOLAOU & ROBERTS (2007) is about 90° to the fault strikes in the region (NW-SE), so the faulting is almost pure dip slip and therefore agrees with the average focal solution in fig. 2. As the data collected by PAPANIKOLAOU & ROBERTS (2007) are on fault scarps younger than 18 ka, there is no evidence for kinematic changes between the 18-ka and the current strain field.

In the foreland area, geomorphic and structural data collected by TONDI *et alii* (2005) on the Mattinata fault showed evidence of right-lateral motion and also suggested that dextral shear characterizes the most recent kinematic behaviour of the structure. As discussed by TONDI *et alii* (2005), earlier left-lateral motion along the Mattinata fault has been inferred mainly from the occurrence of localized, pervasive pressure-solution surfaces, that are consistent with left shear and by the presence of a pull-apart basin, located in a left-stepping overlap zone between two major fault segments of the Mattinata fault. The same authors indicated that the geometry of the stress field currently acting in the area is characterized by a σ1 axis oriented roughly NW-SE and by a σ3 axis trending NE-SW. All these results agree with the current state of stress defined by MONTONE *et alii* (2004) and with the results of the analysis of DEL GAUDIO *et alii* (2007) of focal mechanism data (fig. 2), which established that the seismogenic structures responsible for major earthquakes in the foreland sector of northern Apulia should be sought among transpressive faults with an approximately E-W strike, characterised by dextral movement.

EARTHQUAKE DATASET

A qualitative seismotectonic analysis for each crustal volume was carried out in order to attribute the historical earthquakes to each crustal volume and characterize the historical events with focal depth and kinematics.

Major seismicity in Southern Peninsular Italy, characterized by magnitudes reaching values of 7, is related to seismogenic faults (VALENSISE & PANTOSTI, 2001, and references therein) in an extensional stress field characterized by SW-NE-oriented Shmin-axes (MONTONE *et alii*, 2004; BARBA *et alii*, 2010). Instrumental data show that this seismicity occurs mainly in the first 15 km of the crust (CHIARABBA *et alii*, 2005a). However, some instrumental earthquakes east of this narrow extensional area have hypocentral depths >15 km and strike-slip kinematics. BONCIO *et alii* (2007) pointed out that these pieces of seismic evidence are consistent with a crustal mechanical zoning of the Southern Apennines. The authors suggested that (*i*) the Apennine crust, from the Irpinia seismic zone to the southwest, is characterized by an extensional tectonic regime in the brittle upper crust (up to 15 km depth) overlying a ductile middle and lower crust; (*ii*) the Apulian foreland is characterized by a thick (>20 km), brittle seismogenic crust, including the sedimentary cover and part of the middle crust, which overlies a ductile lower crust; and (*iii*) the zones where the Apennines units overthrust the Apulian crust and where strike-slip seismicity is within the buried foreland are characterized by a complex rheology, with two brittle layers at different depths.

TABLE 3

Dataset of historical earthquakes with moment magnitude ≥4.5 used in this work, whose epicentre are located within the studied area and associated with the four crustal volumes in the model B. Dataset from historical parametric catalogue WORKING GROUP CPTI (2004). The events marked with an asterisk in the column "year", located in the extensional crustal volume (model A), were associated with a transcurrent crustal volume in model B. Moment magnitude uncertainties from WORKING GROUP CPTI (2004) and JENNY *et alii* (2006) are also shown.

Year	Month	Day	Name	Crustal Volume (model B)	LAT	LON	Mw	Mw from CPTI	Mw from Jenny et al. (2006)
99			circello	EXTCV	41.35	14.8	6.3	0.3	0.5
346			sannio	EXTCV	41.38	14.43	6	0.3	0.5
375			benevento	EXTCV	41.13	14.78	6	0.3	0.5
848	6		sannio	EXTCV	41.48	14.27	6	0.3	0.5
989	10	25	irpinia	EXTCV	41.02	15.17	6	0.3	0.5
1120	3	25	rocca d'evandro	EXTCV	41.38	13.92	5.6	0.2	0.5
1125	10	11	sannio-molise	FORECV-N	41.6	15	5.7	0.2	0.5
1139	1	22	benevento	EXTCV	41.129	14.777	4.6	0.1	0.5
1223			gargano	FORECV-N	41.85	16.03	6	0.3	0.5
1273			potenza	EXTCV	40.63	15.8	5.8	0.1	0.5
1293	9	4	sannio	EXTCV	41.3	14.55	5.9	0.1	0.5
1349	9	9	lazio merid.-molise	EXTCV	41.48	14.07	6.6	0.2	0.5
1361	7	17	ascoli satriano	FORECV-N	41.23	15.45	6.1	0.2	0.5
1414			vieste	FORECV-N	41.88	16.18	5.8	0.1	0.5
1456*	12	5	molise	FORECV-C	41.302	14.711	7	0.1	0.5
1456*	12	5	beneventano	FORECV-C	41.15	14.867	6.6	0.3	0.5
1461	6		castelcivita	EXTCV	40.5	15.25	5.2	0.3	0.5
1517	3	17	ariano irpino	EXTCV	41.15	15.08	5.6	0.2	0.35
1560	5	11	barletta-bisceglie	FORECV-C	41.25	16.48	5.7	0.1	0.35
1561	8	19	vallo di diano	EXTCV	40.52	15.48	6.4	0.2	0.35
1627	7	30	gargano	FORECV-N	41.73	15.35	6.7	0.2	0.35
1628	7	12	san severo	FORECV-N	41.685	15.381	4.6	0.1	0.35
1634	11	10	matera	FORECV-S	40.665	16.607	5	0.3	0.35
1646	5	31	gargano	FORECV-N	41.87	15.93	6.2	0.2	0.35
1657	1		apricena	FORECV-N	41.833	15.333	5.2	0.3	0.35
1685	4	25	salerno	EXTCV	40.75	14.75	4.8	0.3	0.35
1688	1	14	pietrelcina	EXTCV	41.2	14.9	4.8	0.3	0.35
1688	6	5	sannio	EXTCV	41.28	14.57	6.7	0.1	0.35
1689	9	21	barletta	FORECV-C	41.272	16.288	5.2	0.3	0.35
1691	9	26	madonna ripalta	FORECV-C	41.25	15.917	4.8	0.3	0.35
1694	9	8	irpinia-basilicata	EXTCV	40.88	15.35	6.9	0.1	0.35
1699			alife	EXTCV	41.333	14.333	4.8	0.3	0.35
1702	3	14	beneventano-irpinia	EXTCV	41.12	14.98	6.3	0.2	0.35
1708	1	26	pollino	EXTCV	39.922	16.126	5.6	0.2	0.35
1712	5	8	campobasso	EXTCV	41.557	14.667	5	0.3	0.35
1713	1	3	massafra	FORECV-S	40.588	17.113	5	0.3	0.35
1714	8		salerno	EXTCV	40.75	14.75	5.2	0.3	0.35
1720	6	7	puglia sett.	FORECV-C	41.261	15.92	5.2	0.2	0.35
1723	6		carinola	EXTCV	41.25	14	4.8	0.3	0.35
1728	2	8	teano	EXTCV	41.283	13.983	5.2	0.3	0.35
1731	3	20	foggiano	FORECV-C	41.27	15.75	6.3	0.2	0.35
1731	10	17	foggia	FORECV-C	41.178	15.999	5.2	0.2	0.35
1732	11	29	irpinia	EXTCV	41.08	15.05	6.6	0.1	0.35
1739	2	13	foggia	FORECV-N	41.5	15.5	5.2	0.3	0.35
1759	5	20	grumento	EXTCV	40.333	15.833	4.8	0.3	0.35
1782	1	12	vitulano	EXTCV	41.167	14.667	4.8	0.3	0.35
1783	11	15	s.severo	FORECV-N	41.667	15.333	5.2	0.3	0.35
1794	6	12	montemarano	EXTCV	41	15	5.2	0.3	0.35
1805	7	26	molise	EXTCV	41.5	14.47	6.6	0.1	0.35
1805	10	13	caiazzo	EXTCV	41.167	14.333	5.2	0.3	0.35
1807	1	28	isernia	EXTCV	41.594	14.231	4.6	0.1	0.35
1807	11	11	tramutola	EXTCV	40.297	15.845	5.2	0.3	0.35
1825	10	27	monteroduni	EXTCV	41.583	14.167	4.8	0.3	0.35
1826	2	1	basilicata	EXTCV	40.52	15.73	5.7	0.1	0.35
1831	1	2	lagonegro	EXTCV	40.082	15.785	5.5	0.1	0.35
1831	11	23	boiano	EXTCV	41.5	14.5	4.8	0.3	0.35
1836	11	20	basilicata merid.	EXTCV	40.15	15.78	5.8	0.1	0.35
1841	2	21	s.marco in lamis	FORECV-N	41.626	15.639	5.4	0.2	0.35
1845	7	10	matera	FORECV-S	40.665	16.607	4.9	0.2	0.35

Continue tab. 3

Year	Month	Day	Name	Crustal Volume (model B)	LAT	LON	Mw	Mw from CPTI	Mw from Jenny et al. (2006)
1846	8	8	campomaggiore	EXTCV	40.53	16.113	5.3	0.2	0.35
1850	11	2	cagnano	FORECV-N	41.817	15.783	4.6	0.1	0.35
1851	8	14	basilicata	FORECV-C	40.95	15.67	6.3	0.1	0.35
1852	4	2	melfi	FORECV-C	41	15.667	4.8	0.3	0.35
1852	12	9	s.severo	FORECV-N	41.667	15.333	5	0.3	0.35
1853	4	9	irpinia	EXTCV	40.82	15.22	5.9	0.1	0.35
1853	6	9	savignano puglia	EXTCV	41.233	15.183	4.8	0.3	0.35
1857	12	16	basilicata	EXTCV	40.35	15.85	7	0.1	0.35
1858	8	6	ricigliano	EXTCV	40.75	15.55	5.2	0.3	0.35
1859	2	4	vietri	EXTCV	40.65	15.517	5	0.3	0.35
1861	11	19	potenza	EXTCV	40.633	15.8	5	0.3	0.35
1864	4	5	s.salvatore	FORECV-N	41.667	15.917	4.8	0.3	0.35
1864	12	28	coppa ferrata	FORECV-N	41.833	15.583	5.2	0.3	0.35
1869	3	31	s.giovanni	FORECV-N	41.717	15.75	5.2	0.3	0.35
1871	8	1	torre mileto	FORECV-N	41.917	15.633	5.2	0.3	0.35
1873	12	13	venafro	EXTCV	41.417	13.967	5.2	0.3	0.35
1875	12	6	s.marco in lamis	FORECV-N	41.689	15.677	6.1	0.2	0.35
1882	6	6	monti del matese	EXTCV	41.55	14.2	5.3	0.1	0.35
1885	9	17	benevento	EXTCV	41.133	14.8	5.2	0.3	0.35
1885	12	26	campobasso	EXTCV	41.543	14.679	5.4	0.2	0.35
1889	12	8	apricena	FORECV-N	41.83	15.692	5.6	0.1	0.35
1892	4	20	gargano	FORECV-N	41.758	16.093	5.2	0.2	0.35
1892	6	6	tremiti	FORECV-N	42.156	15.52	5.1	0.1	0.35
1893	1	25	auletta	EXTCV	40.583	15.417	5.2	0.3	0.35
1893	8	10	gargano	FORECV-N	41.72	16.08	5.4	0.1	0.35
1894	3	25	lesina	FORECV-N	41.867	15.323	5.2	0.3	0.35
1894	5	28	pollino	EXTCV	39.995	16.035	5.1	0.2	0.35
1895	2	1	montesarchio	EXTCV	41.017	14.617	4.8	0.3	0.35
1895	7	19	brienza	EXTCV	40.417	15.7	4.8	0.3	0.35
1896	4	17	monte s.angelo	FORECV-N	41.733	15.967	4.8	0.3	0.35
1897	3	29	venafro	EXTCV	41.5	14.033	4.8	0.3	0.35
1898	11	24	montecalvo	EXTCV	41.233	15	4.8	0.3	0.35
1899	8	16	irpinia	EXTCV	41.143	15.337	4.8	0.3	0.35
1899	10	2	polla	EXTCV	40.555	15.654	4.6	0.1	0.35
1900	12	23	basso adriatico	FORECV-N	41.917	15.333	4.6	0.1	0.35
1902	7	20	mignano	EXTCV	41.383	14	4.6	0.1	0.35
1902	12	16	montesarchio	EXTCV	41.033	14.6	4.6	0.1	0.35
1903	5	4	valle caudina	EXTCV	41.034	14.557	5.2	0.3	0.35
1903	12	7	benevento	EXTCV	41.1	14.767	4.8	0.3	0.35
1904	4	8	gargano	FORECV-N	41.706	15.728	5	0.2	0.35
1904	6	9	venafro	EXTCV	41.467	13.983	4.8	0.3	0.35
1904	7	18	apice	EXTCV	41.1	14.9	5.1	0.1	0.35
1905	3	14	beneventano	EXTCV	40.951	14.805	5	0.1	0.35
1905	6	29	brienza	EXTCV	40.525	15.599	4.8	0.3	0.35
1905	8	18	brancia	FORECV-N	41.7	15.5	4.8	0.3	0.35
1905	11	26	irpinia	EXTCV	41.134	15.028	5.3	0.1	0.35
1906	1	25	bagnoli	EXTCV	40.833	15.033	4.6	0.1	0.35
1906	7	2	montemurro	EXTCV	40.3	16	4.8	0.3	0.35
1907	3	20	castropignano	EXTCV	41.6	14.517	5.2	0.3	0.35
1907	12	18	solofra	EXTCV	40.8	14.9	4.8	0.3	0.35
1908	3	26	miglionico	FORECV-S	40.517	16.55	4.8	0.3	0.35
1909	12	3	castelgrande	EXTCV	40.833	15.4	4.8	0.3	0.35
1910	5	28	s.martino	EXTCV	40.2	16	4.8	0.3	0.35
1910	6	7	irpinia-basilicata	EXTCV	40.9	15.42	5.9	0	0.35
1910	10	3	montemurro	EXTCV	40.283	15.983	5	0.3	0.35
1912	3	17	mercato s.severino	EXTCV	40.8	14.8	4.6	0.1	0.25
1912	7	2	trinitapoli	FORECV-C	41.383	16.133	5.2	0.3	0.25
1913	7	26	lioni	EXTCV	40.883	15.2	4.8	0.3	0.25
1913	10	4	matese	EXTCV	41.513	14.716	5.4	0.1	0.25
1914	12	19	s.agapito	EXTCV	41.583	14.25	5.2	0.3	0.25
1916	6	4	venafro	EXTCV	41.445	13.96	5	0.3	0.25
1917	10	13	castelsaraceno	EXTCV	40.231	16.009	4.8	0.3	0.25
1919	10	21	gargano	FORECV-N	41.671	15.554	5	0.1	0.25
1920	3	7	sant'ilario	EXTCV	40.8	15.7	4.8	0.3	0.25
1921	8	23	mignano	EXTCV	41.4	13.983	4.8	0.3	0.25
1923	11	8	muro lucano	EXTCV	40.677	15.449	5	0.2	0.25
1924	3	26	sannio	EXTCV	41.267	14.764	4.6	0.1	0.25
1924	5	9	solofra	EXTCV	40.895	14.771	4.8	0.1	0.25
1925	7	28	cerignola	FORECV-C	41.264	15.898	4.8	0.3	0.25
1925	8	25	gargano	FORECV-N	41.882	16.179	5.1	0.1	0.25
1927	5	25	cerreto	EXTCV	41.25	14.624	5.2	0	0.25
1927	12	27	deliceto	FORECV-C	41.222	15.386	4.8	0.3	0.25
1930	4	27	salernitano	EXTCV	40.769	14.7	4.7	0.2	0.25

Continue tab. 3

Year	Month	Day	Name	Crustal Volume (model B)	LAT	LON	Mw	Mw from CPTI	Mw from Jenny et al. (2006)
1930	11	6	s.nicola	FORECV-C	41.067	15.7	5	0.3	0.25
1930*	7	23	irpinia	FORECV-C	41.05	15.37	6.7	0	0.25
1931	5	10	s.nicola	FORECV-C	41.067	15.7	4.9	0.1	0.25
1931	11	10	melfi	FORECV-C	41	15.7	4.6	0.1	0.25
1931	12	3	cerignola	FORECV-C	41.26	15.815	4.6	0.1	0.25
1932	3	30	castellaneta	FORECV-S	40.633	16.9	4.9	0.2	0.25
1932	12	3	marsico vetere	EXTCV	40.4	15.8	4.6	0.1	0.25
1933	3	7	bisaccia	EXTCV	41.023	15.351	5.1	0.1	0.25
1934	7	3	s.martino	EXTCV	40.2	16	4.8	0.3	0.25
1935	12	3	calvello	EXTCV	40.467	15.867	4.8	0.3	0.25
1935	12	17	teano	EXTCV	41.3	14	4.8	0.3	0.25
1936	4	3	valle caudina	EXTCV	41.04	14.586	4.6	0.1	0.25
1937	7	17	san severo	FORECV-N	41.785	15.298	5.1	0.1	0.25
1937	12	15	capitanata	FORECV-N	41.704	15.296	4.7	0.1	0.25
1941	5	18	s.severo	FORECV-N	41.7	15.4	4.8	0.3	0.25
1941	8	20	s.severo	FORECV-N	41.7	15.4	5.4	0.1	0.25
1941	9	7	montecalvo	EXTCV	41.2	15	5.2	0.3	0.25
1946	4	3	m.palanuda	EXTCV	39.8	16	4.8	0.3	0.25
1947	7	4	forenza	EXTCV	41.048	15.189	4.8	0.1	0.25
1948	8	18	puglia settent.	FORECV-N	41.58	15.75	5.6	0	0.25
1950	1	1	pietrelcina	EXTCV	41.2	14.9	4.6	0.2	0.25
1950	4	19	pignataro	EXTCV	41.2	14.2	4.8	0.3	0.25
1951	1	16	gargano	FORECV-N	41.808	15.9	5.3	0.1	0.25
1953	7	19	s.giovanni rotondo	FORECV-C	41.357	16.09	4.7	0.1	0.25
1954	8	6	pietragalla	EXTCV	40.667	15.883	5.3	0	0.25
1954	10	26	gargano	FORECV-N	41.8	15.967	4.8	0.1	0.25
1955	2	9	monte s. angelo	FORECV-N	41.72	15.863	5.2	0.1	0.25
1955	7	3	vibonati	EXTCV	40.1	15.7	4.8	0.3	0.25
1955	7	12	s.salvatore	FORECV-N	41.7	15.883	4.8	0.3	0.25
1956	1	9	grassano	FORECV-S	40.57	16.366	5	0.3	0.25
1956	8	17	s.marco	FORECV-N	41.717	15.667	5	0.3	0.25
1956	11	25	macchiagodena	EXTCV	41.583	14.4	4.8	0.3	0.25
1957	5	3	sant'ilario	EXTCV	40.8	15.7	4.6	0.1	0.25
1957	10	19	brienza	EXTCV	40.5	15.7	4.8	0.3	0.25
1960	1	11	roccamonfina	EXTCV	41.283	13.986	5.2	0.3	0.25
1962	1	19	s.marco	FORECV-N	41.667	15.7	4.6	0.1	0.25
1962	8	21	irpinia	EXTCV	41.13	14.97	6.2	0.1	0.25
1963	2	13	tito	EXTCV	40.658	15.782	5.3	0.1	0.25
1964	2	18	savignano puglia	EXTCV	41.167	15.167	4.8	0.2	0.25
1964	6	4	brienza	EXTCV	40.5	15.667	4.8	0.2	0.25
1966	7	6	lucania	FORECV-	40.956	16.194	4.6	0.1	0.25
1966	10	4	picerno	EXTCV	40.6	15.7	4.8	0.3	0.25
1967	6	17	basso adriatico	FORECV-N	41.6	16.2	4.8	0.2	0.25
1967	10	5	carinola	EXTCV	41.25	14.067	5.2	0.3	0.25
1967	12	9	adriatico mer.	FORECV-	41.188	16.457	4.8	0.3	0.25
1968	3	22	montemurro	EXTCV	40.3	16	4.6	0.1	0.25
1969	11	14	polla	EXTCV	40.583	15.567	4.6	0.2	0.25
1970	1	21	basso adriatico	FORECV-N	41.9	16.4	4.8	0.3	0.25
1970	9	27	mignano	EXTCV	41.363	13.986	5	0.2	0.25
1971	5	6	monteleone	EXTCV	41.15	15.233	5.2	0.1	0.25
1971	11	29	marsico	EXTCV	40.5	15.8	4.8	0.1	0.25
1972	2	29	adriatico mer.	FORECV-	41.967	15.383	4.9	0.2	0.25
1973	8	8	vietri	EXTCV	40.65	15.517	5	0.1	0.25
1975	6	19	mattinatella	FORECV-	41.363	16.068	5.1	0.2	0.25
1980	3	9	saracena	EXTCV	39.833	16.133	4.7	0.2	0.25
1980	11	23	irpinia-basilicata	EXTCV	40.85	15.28	6.9	0	0.25
1980	12	3	potenza	EXTCV	40.65	15.75	4.9	0.2	0.25
1981	2	14	baiano	EXTCV	40.985	14.613	4.9	0.1	0.25
1982	3	21	maratea	EXTCV	40.008	15.766	5.2	0.1	0.20
1982	8	15	valle del sele	EXTCV	40.824	15.237	4.8	0.1	0.20
1983	7	27	valle del sele	EXTCV	40.734	15.245	4.5	0.1	0.20
1986	7	23	potentino	EXTCV	40.625	15.671	4.6	0.1	0.20
1988	1	8	appennino lucano	EXTCV	40.13	15.988	4.8	0.1	0.20
1988	4	13	pollino	EXTCV	39.764	16.275	5	0.1	0.20
1990*	5	5	potentino	FORECV-S	40.711	15.299	5.8	0.2	0.20
1990*	5	5	potentino	FORECV-S	40.659	15.88	4.7	0.1	0.20
1991*	5	26	potentino	FORECV-S	40.668	15.803	5.2	0.1	0.20
1992	11	5	manfredonia	FORECV-N	41.562	15.922	4.8	0.2	0.20
1994	10	12	maratea	EXTCV	39.997	15.762	4.8	0.1	0.20
1995	9	30	gargano	FORECV-N	41.754	15.656	5.2	0.2	0.20
1996	4	3	irpinia	EXTCV	40.854	15.293	4.9	0.1	0.20
1997	3	19	matese	EXTCV	41.336	14.705	4.6	0.2	0.20
1998	9	9	appennino calabro-lucano	EXTCV	40.038	15.937	5.7	0.2	0.20
2002	10	31	molise	FORECV-	41.694	14.925	5.8	0.2	0.20

Obviously, assigning the depths of historical earthquakes is highly uncertain, as many authors have mentioned, and the limits of the most common methods are well known (Kovesligethy, 1907; Blake, 1941; Sponheuer, 1960; Shebalin, 1973; Cecic *et alii*, 1996; Gasperini *et alii*, 1999; Gasperini *et alii*, 2010). A significant accuracy of earthquake parameters has only been possible over the last few years, thanks to the increasing number of seismic networks installed all over the world, but in regions characterised by moderate strain rate (about 10^{-9} sec^{-1}), damaging earthquakes (M_w>6) occur with recurrence times longer than hundreds of years. The possibility to retrieve source parameters from the macroseismic fields is crucial in studies of regional seismicity because it allows one to trace the parametric earthquake catalogues back in time, but the common approaches require a considerable amount of subjective judgment.

Recently, Gasperini *et alii* (2010) developed a new method that uses intensity data and associated uncertainties by maximizing the likelihood function of an attenuation equation with observed intensity data to assess the surface (epicentral) and hypocentral (macroseismic depth) location, the physical dimensions and the orientation of the source of historical earthquakes. However, the same authors, testing the method by comparison with reliable instrumental events, showed that the computed macroseismic depths generally underestimate the observations. This result implies that the macroseismic depth inferred by algorithms should still be treated with caution.

Consequently, information about a likely depth range of each event, when no instrumental data are available, has been only qualitatively inferred from the macroseismic field integrated with all available information from the literature. The aim of the following considerations is to determine whether some historical earthquakes traditionally assigned to the extensional belt (i.e., a shallow source) could have a deeper and strike-slip source. Based on this, each historical earthquake was assigned to a specific crustal volume (tab. 3). In tab. 3 an asterisk marks the events with a debated source that are discussed below.

The 1456 earthquakes (fig. 3a)

The 1456 earthquake sequence is the most important in this group of catastrophic events, and its causative source is still debated. The damage area that underwent intensity >VIII effects on the Mercalli-Cancani-Sieberg (MCS) scale of the 1456 sequence is very large (Magri & Molin, 1979; Meletti *et alii*, 1988; Fracassi & Valensise, 2007), extending from central Italy (to the north) to Apulia (in southeastern Italy) and from the Adriatic to the Tyrrhenian coasts. According to the historical catalogue (Working Group CPTI, 2004), the 1456 seismic crisis consists of at least two well-constrained and similarly large mainshocks, the first on 5 December and the second on 30 December (Magri & Molin, 1979; Meletti *et alii*, 1988; Boschi *et alii*, 2000; Guidoboni & Ferrari, 2004; Guidoboni & Comastri, 2005). In the literature, different sources have been proposed for locating the earthquake (see Fracassi & Valensise, 2007 for an exhaustive analysis of the event). Among several others, Sella *et alii* (1988) and Sawyer (2001) proposed a complex southwest-dipping normal-fault system, NW-SE trending, that displaced the Apulian platform beneath the Apennine wedge as a causative source. Recently, Fracassi & Valensise (2007) suggested that

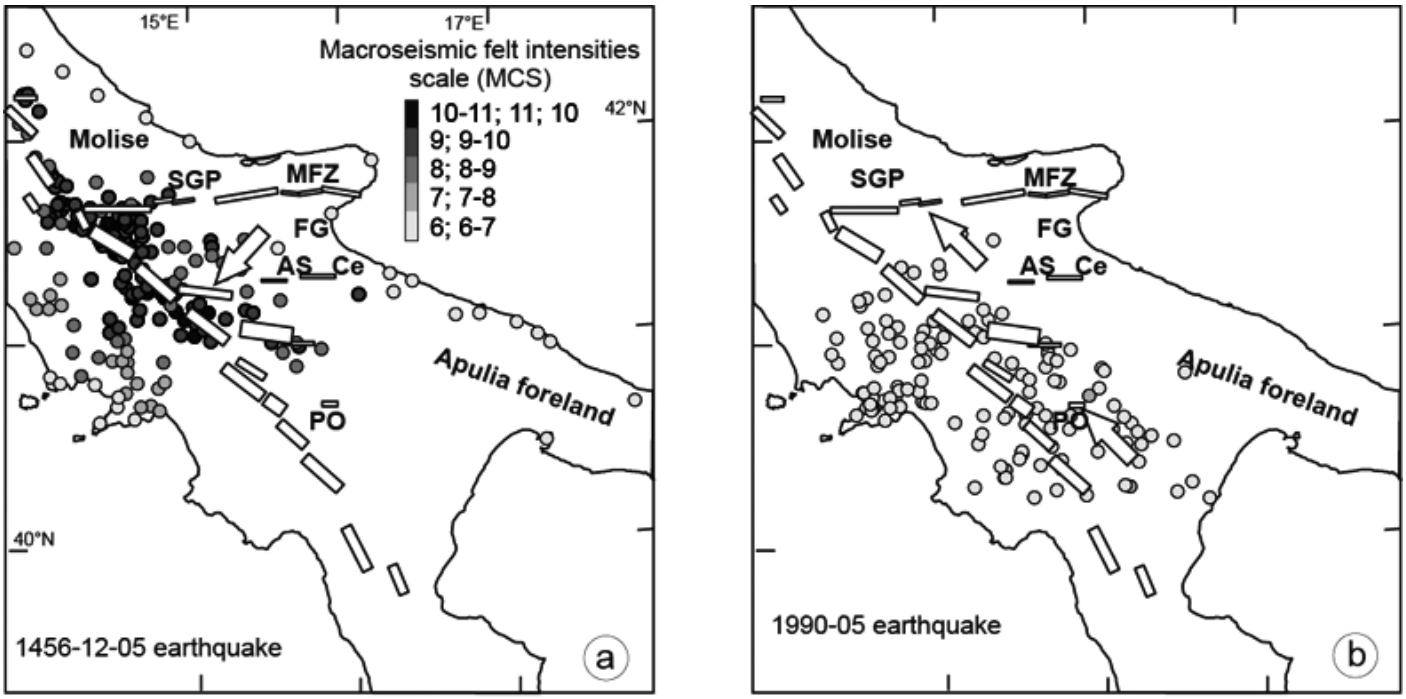

Fig. 3 - Macroseimic fields of intensity data of some historical earthquakes from DBMI04 (Stucchi *et alii*, 2007). The white boxes represent individual seismogenic faults (from Basili *et alii*, 2008), and the large arrows identify the source responsible for the event shown. Key: MFZ = Mattinata fault zone; PO = Potenza; SGP = San Giuliano di Puglia; As = Ascoli Satriano; FG = Foggia; Ce = Cerignola.

these multiple events were generated and/or controlled by the oblique right-lateral reactivation of discrete segments of regional deeper (between roughly 10 and 25 km), E-W seismogenic faults. Concerning the kinematcs, Fracassi & Valensise (2007) hypothesized that one of the 1456 sources forms the westernmost part of an E-W seismogenic shear zone extending from the Apulia foreland to the Apennines. In accordance with Fracassi & Valensise (2007), the 1456 earthquake sequence was associated with EW strike-slip sources of the foreland crustal volume.

The 1990 Potenza seismic sequence (fig. 3b)

Boncio *et alii* (2007) revised the aftershock sequences of two moderate-magnitude, right-lateral strike-slip earthquakes that occurred at deep crustal levels in the Potenza area (May 1990, M 5.7, and May 1991, M 5.2). Their analysis provided new constraints on the strike-slip stress regime acting in the source region (N142°-trending deviatoric compression and N232°-trending deviatoric tension). The sequence depth ranges between 15 and 25 km.

The 1930 Irpinia earthquake

The early instrumental 1930 earthquake occurred a few tens of kilometres to the north of the epicentral area of the 1980 Irpinia earthquake and has been recently studied by Pino *et alii* (2008), who performed a waveform modeling of historical seismograms of this earthquake. Their results indicate that the 1930 event nucleated at ~14 km depth and ruptured a north-dipping, N100°E-striking plane with an oblique motion.

Therefore, even if this earthquake is located within the extensional area of the Southern Apennines, it shows seismotectonic features compatible with the foreland tectonics setting. Then, to estimate the influence of the 1930 and 1990 earthquakes in terms of deformation rates, in model A they were assigned to the extensional crustal volume, and in model B to the foreland crustal volume, following their inferred hypocentral depths.

Estimation of the magnitude-frequency distribution

The seismicity catalogues provide estimates of short-term (Catalogo della Sismicità Italiana, Castello *et alii*, 2005, about 20 years) and relatively long-term (historical catalogue, Catalogo parametrico dei Terremoti Italiani, Working Group CPTI, 2004, about 1000 years) seismic-moment rates. To accurately estimate the seismic budget of active crustal deformation, the historical Working Group CPTI (2004) catalogue was used and the cumulative Gutenberg-Richter (1944) magnitude-frequency distribution was calculated (hereinafter, GR) expressed as $\log N(M) = a - bM$, where N is the cumulative frequency of earthquakes with magnitudes larger than M per year, a is the recurrence rate of the smallest events and b represents the slope of the curve (slopes in fig. 4). Magnitude-frequency distributions are determined for each crustal volume and for models A and B, as previously defined, taking into account uncertainties of the completeness interval and magnitude errors. Statistical analysis of the historical catalogue (Pace *et alii*, 2006) suggested that the catalogue is complete for Mw>5.5 from 1600 A.D. and for Mw>6.4 from 1000 A.D. However, Jenny *et alii* (2006) discussed how the historical dataset does not allow an unequivocal assessment of the completeness interval and that the best estimates of the seismic deformation for Southern Italy use a shorter completeness interval. Some preliminary tests of the moment rate estimation in the extensional crustal volume, using the two completeness intervals and the errors involved in the magnitude estima-

tion, as proposed by the PACE *et alii* (2006) and JENNY *et alii* (2006), have shown a sensible difference. The use of completeness intervals proposed by JENNY *et alii* (2006) returns the highest value of the moment rate, about 30×10^{16} Nma^{-1}, whereas the use of completeness intervals as proposed by PACE *et alii* (2006) returns a value of about 7×10^{16} Nma^{-1}. Therefore, following JENNY *et alii* (2006), a completeness interval was assigned starting from 1000 A.D±200 to the events with M≥7.0, 1475±125 to the earthquakes with 6.5≤Mw<7, 1625±100 to the earthquakes with 5.5≤Mw<6.5, 1780±80 to the earthquakes with 5.5≤Mw<6, 1870±40 to the earthquakes with 5.0≤Mw<5.5 and 1885±20 to the earthquakes with 4.5≤Mw<5.

To evaluate the influence of the uncertainty in the earthquake-crustal volume assignment in GR parameters and consequently in the deformation rates, the following computational tests were performed, varying the volumes and the earthquakes associated with them.

Model A: starting from the historical earthquake dataset (fig. 1), on the basis of a plan view, I divided the earthquakes that occurred in the extensional (EXTCV) or in the foreland (FORECV-N, FORECV-C and FORECV-S) crustal volumes, respectively (GR a, c, d and f in fig. 4).

Model B: I moved those events that, even if located in the EXTCV, were associated with strike-slip tectonics in the underlying crust and discussed in Section 4.3. In particular, in Model B, I associated with the FORECV-C the two 1456 December shocks and with the FORECV-S the 1990 and 1930 earthquakes (GR b, e and g in fig. 4).

Successively, using a Monte Carlo simulation method (described in the Section 3), with errors in the magnitude estimation and completeness intervals, I estimated the standard deviations of the GR slopes by simulating 10,000 catalogues for each of the four crustal volumes and for each of the earthquake-source association models, for a total of 7 simulations (fig. 4). Grey areas drawn above the slopes in fig. 4 graphically represent the computed ranges of uncertainties.

Finally, the integration of these distributions returns a moment-rate estimate that provides a slip rate by using equations (1)-(4).

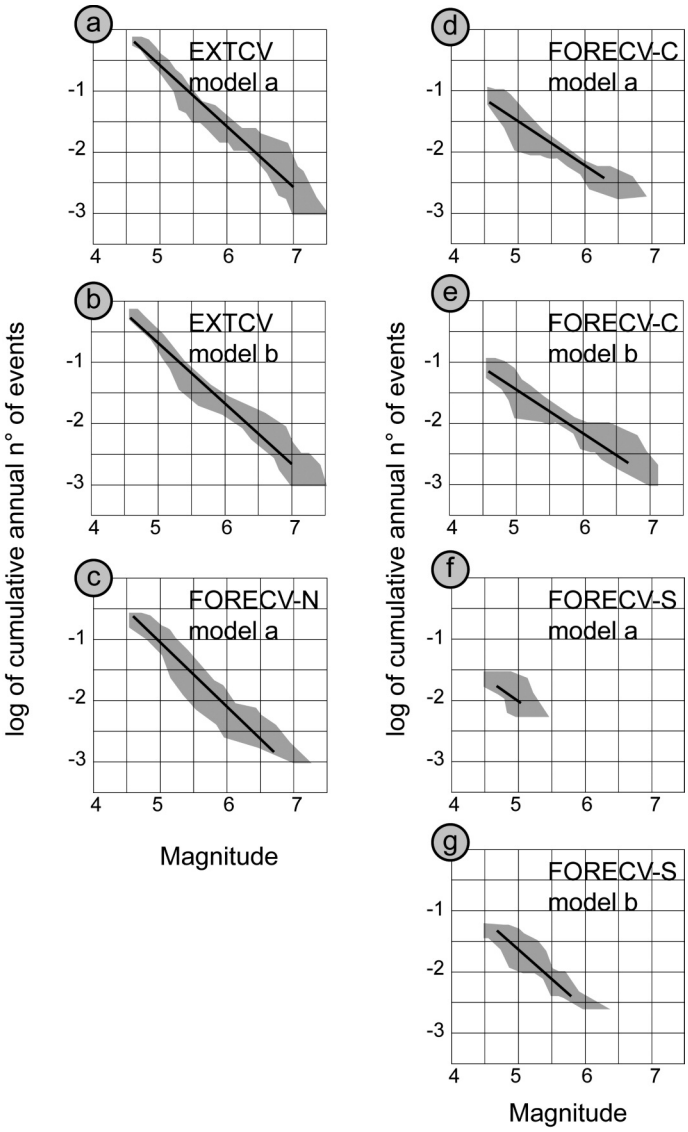

Fig. 4 - Gutenberg-Richter slopes based on the earthquakes listed in tab. 1, with exclusion of the events from the interval of catalogue completeness. For each crustal volume (except the FORECV-N), the two different GR slopes were referred to the models (model A and B) discussed in the text. The grey areas represent the uncertainty range owing to the errors associated with magnitudes and completeness length of the catalogues, as calculated in this work.

COMPUTATIONAL STEPS

The rates of seismic moment released for each crustal volume and the components of the slip rate vector were estimated by using equations (1)-(8). The errors that can affect the calculation of the seismic moment rate were in the estimation of the Gutenberg-Richter parameters, in the assumptions of the coefficients of the KANAMORI & ANDERSON (1975) relationship and in the maximum magnitude evaluation. Moreover, in the computation of the slip rate the errors in the value of the shear modulus, in the estimation of the length and seismic thickness and in the definition of the kinematics also have to be taken into account.

The seismic moment rate is, in fact, constrained by five parameters (Eqs. 5-8): a and b (coefficients of the magnitude-frequency distribution of earthquakes), c and d (coefficients of the magnitude-moment relationship) and M_{max} (maximum magnitude); the slip rate required five extra parameters (equations (1)-(4)): dip and rake (focal mechanism), μ (shear modulus), L1 (length of the crustal volume) and L3 (seismic thickness). According to MAZZOTI & ADAMS (2005), three main classes can be used to group these parameters: (1) the uncertainty is aleatory and derived from a formal fit to a data set (can be described by a standard deviation about a mean); belonging to this class are the a and b Gutenberg-Richter coefficients and dip and rake of the assumed average focal mechanism; (2) the uncertainty is aleatory, derived from data analysis, but also involves some degree of subjectivity in its definition; this class includes the maximum magnitude of each crustal volume (Mmax), to which I assigned the error given in JENNY *et alii* (2006), the length of the seismic zone (L1, measured by GIS software) and the shear modulus (μ, 3.0 10^{10} Pa based on a typical range for crustal rocks, TURCOTTE & SCHUBERT, 2002), to both of which I assigned a 10% uncertainty, and the magnitude-moment relationship parameters (c and d), to which I assigned a value of 0.1 of uncertainty; (3) the uncer-

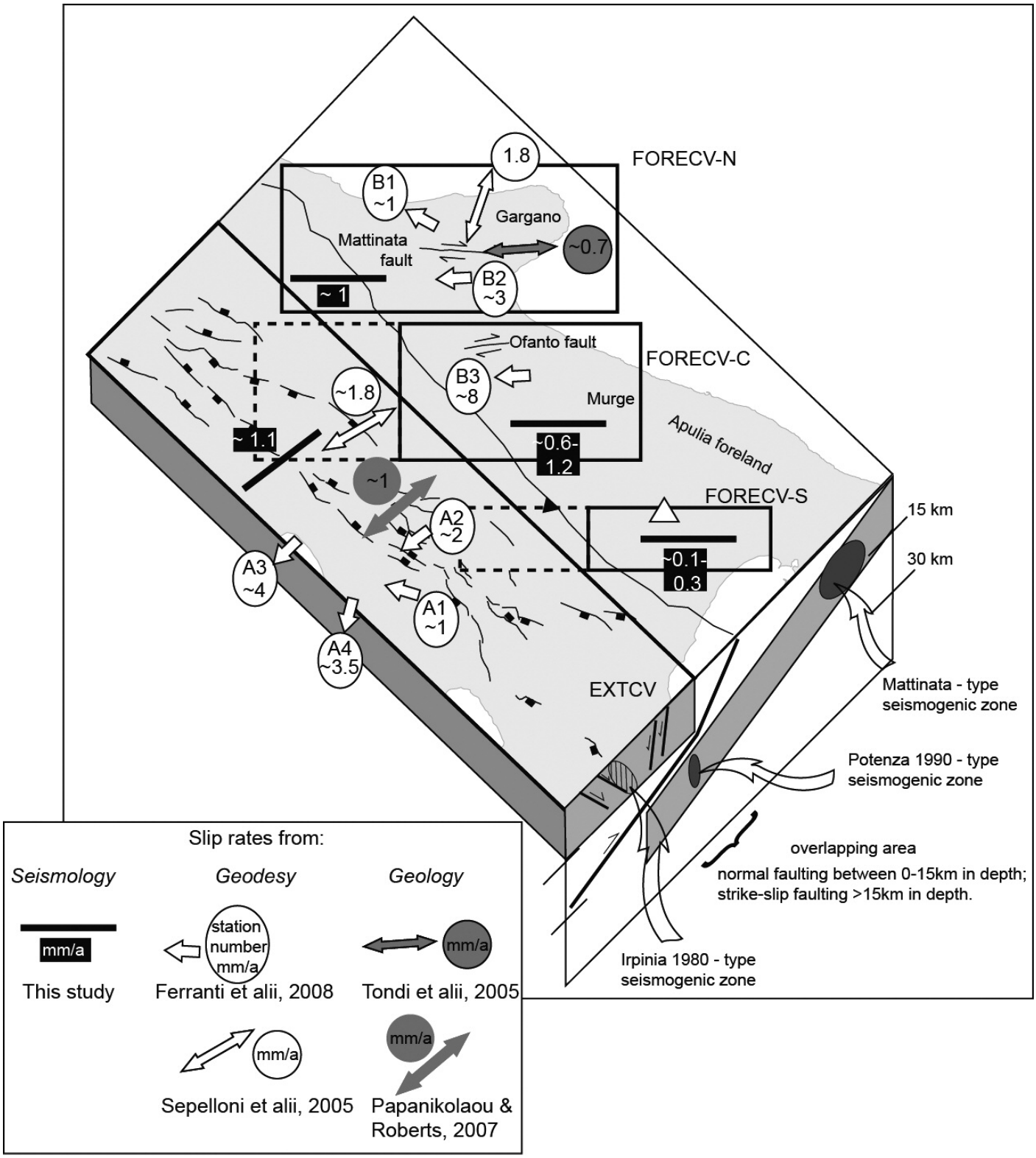

Fig. 5 - Seismic slip rates obtained for the crustal volumes (black arrows), compared with those derived from geodetic (white arrows) and geological (grey arrows) studies. The values from FERRANTI *et alii* (2008) are computed with MATE (white triangle) held fixed. The values are in mm/a.

tainty is epistemic, mostly due to a lack of knowledge of the underlying process (to which I assigned a conservative 30% of uncertainty); to this class belongs the seismic thickness (L3) because of the lack of systematic studies on the definition of the average seismic thickness and relative errors, at least in this sector of the Apennines.

Once the mean values of all the parameters and their ranges of variability are defined, the uncertainties in the values of the seismic moment rates and observed velocities for each crustal volume are estimated by applying a Monte Carlo simulation method. Assuming random errors in these parameters, with known medians and

standard deviations, Gaussian deviates can be introduced. If m is the vector of mean values of the parameters, the new vector P = (a, b, c, d, M_{max}, μ, L1, L3, dip, rake) can be iteratively obtained using:

$$P = Cz + m \tag{9}$$

where z is the standard Gaussian random vector, with deviates produced using the polar Box-Mueller transform, and C is the Cholesky decomposition of the covariance matrix of the parameter vector V (symmetric and positive definite matrix), with a unique lower triangular matrix such that $V = C \times CT$.

Where the V diagonal elements are the σ^2 of each parameter.

Because some of the parameters used are correlated, the covariance matrix, V, is non-diagonal, and it is necessary to compute the covariance's σab and σcd considering the calculated correlation coefficient, r_{ab}, and assuming r_{cd} is equal to 0.95, as proposed by PAPAZACHOS & KIRATZI (1992). Using equation (9), the new parameters can be obtained in each iteration to estimate the new value of $\dot{M}o$ and the corresponding slip rate. This set of values can be used to obtain the mean and standard deviation.

Table 2 and fig. 5 summarize the input parameters and the results of such analysis.

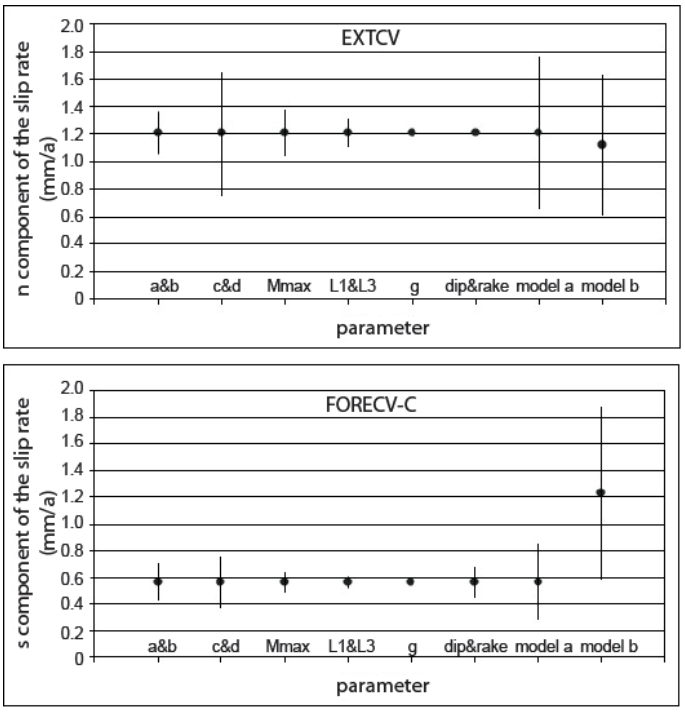

Fig. 6 - Contribution of parameter sets to final deformation uncertainty. Examples of the EXTCV (upper graph) and FORECV-C (lower graph). Circles and error bars represent the contribution of each parameter (x-axis) set on uncertainty in deformation rate estimate (y-axis).

RESULTS

The results in the deformational pattern obtained for each model are shown in tab. 2. In particular, in tab. 2, the G-R parameters, $\dot{M}o$, and velocities as computed by eqs (2-4) are given in terms of mean values and standard deviations. Moreover, for a meaningful representation of the velocity field, the highest components of the slip rate vectors are synthetically illustrated in fig. 5. Principal results of the computed deformational pattern for each model are given below.

Regarding the EXTCV, the calculated crustal extensional rate along a NE-SW direction (normal component of the slip rate vector) for the models A and B are 1.21±0.55 mm/a and 1.12±0.51 mm/a, respectively.

In the FORECV-N, the along-strike component of the slip rate vector is 0.96±0.54 mm/a. Considering the available seismotectonic data, I did not define a model B for this crustal volume.

Regarding the FORECV-C, the calculated main deformation rate is 0.56±0.28 mm/a for the model A. Using the model B, an increasing value in the L1 dimension, combined with the increased maximum magnitude occurred within the volume, allowed an along strike deformational axis of 1.23±0.64 mm/a to be estimated.

In the FORECV-S, the along-strike deformational axis for the model A is 0.3±0.1 mm/a. This value was obtained after fixing b to be equal to 1.0 with an uncertainty of 0.1. This was necessary because the limited range of magnitude of the earthquakes that occurred within this crustal volume did not allow any significant statistics. For this crustal volume, the model B is particularly important regarding the L1 dimension, as well as the possibility of expanding the magnitude range of the events located within the FORECV-S. The computed along strike deformational axis, using the model B, is 0.11±0.05 mm/a.

DISCUSSION

EFFECTS OF THE INPUT DATA

The results show that the rates of the seismic deformation are influenced by the variations in shape, dimension and associated earthquakes of the crustal volume undergoing deformation. To illustrate this influence, I computed the coefficients of the GR relationship, the seismic moment rate and the rates of deformation in the Southern Apennines of Italy. The results contain the uncertainty and errors associated with the entered data, especially with catalogue completeness and quality, focal mechanism dataset, size and shape of the seismogenic volume.

By analyzing the effect of each parameter and the influence of the earthquake association with the crustal volume to the final uncertainty, it is possible to highlight some targets for future improvement of the seismic deformation estimates. Fig. 6 shows such analysis for the Southern Apennines crustal volumes. For each of the input parameters, I varied the values between the standard deviation while the other parameters were fixed to the mean value (the procedure is the same as described in section 3 but uses a simplified vector of the parameters containing only the investigated parameter). Starting from model A, I calculated upper and lower slip rates in order to indicate the contribution of each parameter to the final uncertainty estimates and evaluate the weight of each of them in the sum of variances uncertainty. As shown on fig. 6, the parameters with the largest contribution are the coefficients of the magnitude-moment conversion (c and d). The uncertainty of the c and d coefficients can contribute, alone, an error of 34-37% in the

final values and represents the main source of error, with weights in the range of a 40 to 49% contribution to the total error.

The impact of this parameter is almost twice as large as that of the second and third contributors, magnitude-frequency (a and b) and maximum magnitude (M_{max}). The magnitude-frequency coefficients, which themselves bring errors and uncertainties in the historical catalogues, can contribute to an error of 13 to 24% and weight from 17 to 28% in the overall source of uncertainty. The maximum magnitude leads to a 13% uncertainty in the final values, and weights of a maximum of 18% in the sum of the variances uncertainty.

Geometrical and kinematics parameters (L1 and L3, dip and rake), as well as the rheological parameter g, have minor effects. Together, they are able to contribute a maximum of 13% to the final uncertainty and account for 15-17% of the sum of each variable.

Moreover, these errors could be sensibly reduced by improving seismological and rheological studies as well as the quality of records of the minor seismicity of the instrumental earthquake catalogues. Conversely, because of the long recurrence time of large events, improvements to the Kanamori and Anderson relation are more likely to come from theoretical studies (e.g., Atkinson & Boore, 1987) rather than from a significant increase in the number of events defining the empirical relation. According to Mazzotti & Adams (2005), the uncertainty contributions from a and b and the maximum magnitude M_{max} are related to the understanding of the physical processes controlling the magnitude distribution of large events in intraplate regions, but I stress that also the quality, in terms of magnitude estimation and completeness, of the earthquake catalogues plays an important role, as discussed in section 2.4.

Furthermore, the effect of the crustal-model geometry definition on the evaluation of the seismic budget of active crustal deformation has an influence at least comparable to the parameter uncertainties, as is evident from the difference in the values of the models A and B shown in fig. 6. Even if the EXTCV shows a quite stable result after moving some historical events, the FORECV-C returns an about double value in model B in respect to model A. This implies that accurate seismotectonic studies and quantitative parameter estimation of historical earthquakes need to be taken into account for computing active crustal deformation.

Seismotectonic considerations

As shown in fig. 1, most of the recent seismicity is concentrated in a narrow belt along the core of the Apennines, as are most of the historical sources, which appear to be associated with NW-SE-trending normal faults. The results of this work reinforced and confirmed the existence, in the Southern Apennines, of high extensional values of crustal deformation (e.g., Westaway, 1992; Selvaggi, 1998; Jenny *et alii*, 2006). For this region, previous investigators have calculated the rate of extension on the basis of moment-tensor summation. Among others, Westaway (1992) evaluated extensional rates up to 5 mm/a, whereas Selvaggi (1998) and Jenny *et alii* (2006) computed extensional rates of about 1.6 mm/a and 2 mm/a, respectively. Moreover, Jenny *et alii* (2006), using geodetic data, computed extensional rates of ~3 mm/a. Assuming a direction of maximum extension about a NE-SW orientation, values of about 1 mm/a have been computed in the present work.

Moreover, in this work, a more complex tectonic model was taken into account, with four crustal volumes characterized by two different kinematic styles. In fact, given the availability of recent focal mechanism solutions (e.g. Pondrelli *et alii*, 2006; Del Gaudio *et alii*, 2007) and new geodetic (e.g. Serpelloni *et alii*, 2005; Devoti *et alii*, 2008; Ferranti *et alii*, 2008; Caporali *et alii*, 2011) and numerical simulation (e.g. Barba *et alii*, 2010) data, a discriminated between an extensional crustal volume in the western part of the Southern Apennines and a transcurrent regime in the eastern area was applied.

Other studies based on permanent and temporary GPS measurements show that the velocity field in southern Italy is consistent with the described tectonic setting (e.g. Serpelloni *et alii*, 2005; Devoti *et alii*, 2008; Caporali *et alii*, 2011). In general, active strain rates computed across the extensional area of the Southern Apennines through the analysis of geodetic data (Serpelloni *et alii*, 2005; Jenny *et alii*, 2006; Devoti *et alii*, 2008; Ferranti *et alii*, 2008; Caporali *et alii*, 2011) and geological data (Papanicholau & Roberts, 2007) indicate velocities that are, on average, of the same order of magnitude as those obtained from seismic data. On the contrary, geodetic strain rates computed across the foreland of the Southern Italy excess the seismic and geologic rates (Tondi *et alii*, 2005). In addition to geometrical problems and short time-series of geodetic data, the partial seismic deficit, following D'Agostino *et alii* (2008), could be resolved considering that (*i*) a large part of the total deformation is expressed aseismically, or (*ii*) seismic deformation could be driven by small-scale tectonic processes (Selvaggi, 1998; Papanikolaou *et alii*, 2005). Finally, the possibility of a large amount of seismic release in the near future cannot be ruled out.

In fig. 5 the velocity vectors computed by Serpelloni *et alii* (2005) indicate an extensional velocity of ~1.8 mm/a along the axis of the belt in an ENE-WSW direction, but a similar velocity field is computed for the Gargano area along a mean NE-SW direction.

Devoti *et alii* (2008) presented a velocity field of the Italian area derived from continuous GPS observations from 2003 to 2007. Although the aim of Devoti *et alii* (2008) paper was to provide further constraints on the kinematics of the Apennines subduction, useful data on the velocity of extension along the Apennines can be extracted. Devoti *et alii* (2008) described that the extension smoothly starts near the north-eastern margin of the Tyrrhenian Sea, reaching a maximum of about 2 mm/yr. Southernmost, crossing the Tyrrhenian Sea and the central and southern Apennines, the extension reaches its maximum value, about 3-4 mm/yr.

Recently, Caporali *et alii* (2011), basing on about one hundred of permanent GPS stations, computed a new strain field for the Italian territory. By using a weighted summation over the local velocity data, Caporali *et alii* (2011) obtained the geodetic shear strain rate for several area corresponding to the seismogenic zones (ZS) of the Working Group MPS (2004). Applying the Savage & Simpson (1997) relationship, slip rates were estimated in four of the ZS studied by Caporali *et alii* (2011), roughly coinciding with the four crustal volumes. In the extensional area ZS 927 (for details see tab. 1 in Caporali *et*

alii, 2011), using the same kinematics of the EXTCV and by means of eq. (3), a slip rate was estimated of about 1 mm/a, which is very close to the seismic velocity obtained for the EXTCV. Conversely, the velocity along strike obtained for three ZSs (924, 925 and 926 in CAPORALI *et alii*, 2011), using he same kinematics of FORECVs, and by means of eq. (4), returned values six times greater than the seismic velocities. Because ZSs 924, 925 and 926 have dimensions quite similar to FORECV-N, FORECV-C and FORECV-S, it was recognized that a large amount of the differences between the geodetic and seismic velocities is due to the sparse order distribution and the exiguous number of the GPS sites within the Apulia foreland. Actually, CAPORALI *et alii* (2011) computed geodetic strain rate in the ZS 924 using 11 GPS station, whereas the ZSs 924, 925 and 926 contain 5,4 and 7 GSP station, respectively. At least in these areas, further advance in the GPS network could be certainly help to depict more robust strain fields.

At a more local scale, FERRANTI *et alii* (2008) addressed the interseismic deformation of the Southern Apennines by analyzing new campaign GPS velocities. The observed displacements suggest active extension to the west and transpression in the east. Their GPS solutions for the extensional belt of Southern Apennines suggest NE-SW directed extension (fig. 5; sites A1-A4 with the International GPS System permanent site MATE held fixed). When viewed relative to MATE sites located on the western part of the extensional area move toward the southwest at rates which increase from ~1 mm/a to ~3.5 mm/a from east to west (fig. 5). In particular, the scalar velocities of the more easterly sites (A1 e A2, fig. 5) are broadly compatible with the extensional rates derived from historical seismicity in this paper (~1 mm/a for the EXTCV), whereas the two westernmost sites (A3 and A4 in fig. 5), indicate rates of extension of ~3-4 mm/a.

FERRANTI *et alii* (2008) also shown that the eastern Apulia sites in Gargano and northern Murge are moving westward relative to MATE with velocities of ~8 mm/a (site B3 in Murge), ~5 mm/a (site B2 in Gargano) and ~3 mm/a (site B1 in Gargano). The authors suggested that the progressive northerly decrease in westward motion of sites B3, B2 and B1, relative to MATE, is accommodated along ~east-west trending strike-slip faults mapped or inferred across these sites. About 5 mm/a differential displacement between B3 and B2 must be accommodated by structures buried beneath the Ofanto valley (Ofanto fault in fig. 5 or sub-parallel faults). Further to the north, differential motion between sites B1 and B2, straddling across the western part of the east-west striking Mattinata Fault (fig. 5), which dissects the Gargano block, yields an estimation of ~2 mm/a maximum right-lateral slip. This result yields a difference of ~1 mm/a with the rate computed for the FORECV-N along an E-W direction. Conversely, a difference of about 3-4 mm/a is observed between the differential displacement between B3 and B2 and the FORECV-C value. However, because the volumes used to compute active seismic deformations are different from the area covered by the geodetic network (see fig. 5), it is possible to hypothesize along and/or across strike variation of seismic release properties within the volumes, with areas of larger fraction of accumulated deformation released aseismically.

The comparison of the present seismic crustal deformation rates with the long-term geologic strain rates is obviously difficult, because geological data generally refer to a fault or a fault system, whereas seismic crustal models provide results for a crustal volume that could include other faults; but geological data offer the advantage of including several seismic cycles, so they show a reliable long-term average deformation rate. Velocity and strain fields have been constructed from measurements of striated faults offsetting Late Pleistocene and Holocene features (PAPANIKOLAOU & ROBERTS, 2007; TONDI *et alii*, 2005). Particularly, PAPANIKOLAOU & ROBERTS (2007) computed the cumulative throw and throw-rate profiles along a 170-km normal fault system, roughly coincident with the EXTCV as defined in the present work. They show that the cumulated throw-rate curve has a number of local maxima and minima, but overall the summed profiles resemble that for a single fault, as the maxima occur close to the centres of the profiles, consistent with interaction between these crustal-scale faults. They computed a maximum value of 1.1±0.25 mm/a for the extensional rate by assuming 45° fault dips.

In the FORECV-N area, right-lateral motion along the Mattinata fault system has been studied by TONDI *et alii* (2005). The authors, by integrating the results of palaeoseismological data, giving 0.2-0.3 mm/a for the vertical component of motion (which they estimated to be about 1/4 of the horizontal component), and those derived from mesostructural analysis, inferred a dextral shear slip-rate of 0.7-0.8 mm/a.

CONCLUSIONS

Drawing from seismicity catalogues, the rates of seismic moment release were computed together with the seismic slip rates in seismic zones of southern Italy. Geological and geophysical data indicate that the region can be divided into four broad crustal seismogenic volumes: an extensional crustal volume in the western part and three transcurrent crustal volumes in the eastern area. For each crustal volume, the seismic moment rates are computed by integrating magnitude-frequency relations of historical earthquakes. Finally, because the seismic slip rate on a fault is proportional to the seismic moment release, knowledge on the tectonic style of an area allow to estimate the horizontal and vertical components of the seismic slip rate.

With the aim of evaluating how deformational-rate estimates can be affected by variations of the modeled crustal volumes, the geometry of the volumes was changed. In a first step the overlapping of the volumes was excluded using a 2D plan view to extract earthquakes falling inside each crustal volume, whereas in the following models the overlapping was accounted for, and consequently, for the events inside this area of superposition, a qualitative choice was carried out, based mainly on the available macroseismic data, to define their crustal volume of appurtenance. The main results of this research may be summarized as follows:

1) The deformational pattern indicates the dominance of extensional stress in the axial zone of the Southern Apennines, with the direction of maximum extension almost NE-SW and velocity of about 1 mm/a. In the foreland domain, the deformational style is transcurrent, with the principal deformational axes trending ~E-W and velocity ranging between 0.1 and 1.2 mm/a.

2) The errors that affect the estimate of the crustal deformation using the seismicity catalogues may be significant. These errors contribute to possible restrictions on the validity of the adopted formulas as well as to uncertainties in the parameters used, which include the completeness and quality of the seismological record. The parameters with by far the largest contribution are the coefficients of the magnitude-moment relationship; the second and third contributors are the coefficients of the magnitude-frequency distribution and the maximum magnitude. Uncertainties in the geometrics and kinematics parameters have minor effects.

3) Furthermore, the effects of the crustal model (and the consequent earthquake association) are in the same order as the uncertainties of the parameters involved in the computation.

4) Even if the use of historical earthquakes suffers from the intrinsic limitations of a qualitative and interpretive association of focal parameters, with the need for caution in interpreting the results, the estimated crustal deformation is quite close to the geodetic and geological values.

Overall, the computed deformational rates confirm the importance of the use of active tectonic terms for the Southern Apennines in the recent literature, thus highlighting the high seismogenic potential for the area with strong seismic-hazard implications.

ACKNOWLEDGEMENTS

I wish to thank Bruno Pace for useful, friendly and stimulating discussions at different stages of the paper. The anonymous reviewers, the Associate Editor Daniela Pantosti and the Editor in Chief Sandro Conticelli, are kindly acknowledged for their critical reading of the manuscript and for their valuable suggestions. The work was partially supported by "Fondi d'Ateneo ex 60%", B. Pace responsible.

REFERENCES

ALLMENDINGER R. (2001) - FaultKinWin, www.geo.cornell.edu/geology/faculty/RWA/programs.html

AMATO A. & MONTONE P. (1997) - *Present-day stress field and active tectonics in southern peninsular Italy.* Geophys. J. Int., **130**, 519-534.

AMATO A. & SELVAGGI G. (1993) - *Aftershock location and P-velocity structure in the epicentral region of the 1980 Irpinia earthquake.* Annali di Geofisisca, **36**, 3-15.

ANDERSON H. & JACKSON J. (1987) - *Active tectonics of the Adriatic region.* Geophysical Journal of the Royal Astronomical Society, **91**, 937-983.

ATKINSON G.M. & BOORE D.M. (1987) - *On the m_N, M relation for eastern North American earthquakes.* Seismol. Res. Lett., **58**, 119-124.

AZZARA R., BASILI A., BERANZOLI L., CHIARABBA C., DI GIOVAMBATTISTA R. & SELVAGGI G. (1993) - *The seismic sequence of Potenza (May 1990).* Annali di Geofisica, **36**, 237-243.

BARBA S., CARAFA M., MARIUCCI M.T., MONTONE P. & PIERDOMINICI S. (2010) - *Present-day stress-field modelling of southern Italy constrained by stress and GPS data.* Tectonophysics, **482**, 193-204.

BARCHI M., AMATO A., CIPPITELLI G., MERLINI S. & MONTONE P. (2006) - *Extensional tectonics and seismicity in the axial zone of the Southern Apennines.* Boll. Soc. Geol. It., **7**, 47-56.

BASILI R., VALENSISE G., VANNOLI P., BURRATO P., FRACASSI U., MARIANO S., TIBERTI M.M. & BOSCHI E. (2008) - *The Database of Individual Seismogenic Sources (DISS), version 3: Summarizing 20 years of research on Italy's earthquake geology.* Tectonophysics, **453**, 20-43.

BENEDETTI L., TAPPONI, P., KING G. & PICCARDI L. (1998) - *Surface rupture of the 1857 southern Italian earthquake.* Terra Nova, **10**, 206-210.

BERNARD P. & ZOLLO A. (1989) - *The Irpinia (Italy) 1980 earthquake: detailed analysis of a complex normal faulting.* J. Geophys. Res., **94** (B2), 1631-1647.

BILLI A. (2003) - *Solution slip and separations on strike-slip fault zones: theory and application to the Mattinata Fault, Italy.* J. Struct. Geol., **25**, 703-715.

BLAKE A. (1941) - *On the estimation of focal depth from macroseismic data.* Bulletin of the Seismological Society of America, **31**, 225-231.

BONCIO P., MANCINI T., LAVECCHIA G. & SELVAGGI G. (2007) - *Seismotectonics of strike-slip earthquakes within the deep crust of southern Italy: Geometry, kinematics, stress field and crustal rheology of the Potenza 1990-1991 seismic sequences (Mmax 5.7).* Tectonophysics, **445**, 281-300.

BOSCHI E., GUIDOBONI E., FERRARI G., GASPERINI P., MARIOTTI D. & VALENSISE G. (2000) - *Catalogo dei forti terremoti in Italia dal 461 a.C. al 1997.* Annali di Geofisica, **43**, 843-868 and CD-ROM.

BROZZETTI F. (2011) - *The Campania-Lucania Extensional Fault System, southern Italy: A suggestion for a uniform model of active extension in the Italian Apennines.* Tectonics, **30**, TC5009. doi: 10.1029/2010TC002794.

BULL J.M., BARNES P.M., LAMARCHE G., SANDERSON D.J., COWIE P.A., TAYLOR S.K. & DIX J.K. (2006) - *High-Resolution Record of Displacement Accumulation on an Active Normal fault: Implications for Models of Slip Accumulation during Repeated Earthquakes.* J. Struct. Geol., **28** (7), 1146-1166.

CAPORALI A., BARBA S., CARAFA M., DEVOTI R., PIETRANTONIO G. & RIGUZZI F. (2011) - *Static stress drop as determined from geodetic strain rates and statistical seismicity.* J. Geophys. Res., **116** (B2), B02410. doi: 10.1029/2010JB007671.

CASTELLO B., SELVAGGI G., CHIARABBA C. & AMATO A. (2005) - *CSI Catalogo della sismicità italiana 1981-2002, version 1.0.* INGV-CNT, Rome, http://www.ingv.it/CSI/.

CECIC I., MUSSON R. & STUCCHI M. (1996) - *Do seismologists agree upon epicentre determination from macroseismic data? A survey of the ESC "macroseismology" working group.* Ann. Geofis., **39** (5), 1013-1027.

CELLO G., TONDI E., MICARELLI L. & MATTIONI L. (2003) - *Active tectonics and earthquake sources in the epicentral area of the 1857 Basilicata earthquake (southern Italy).* J. Geodyn., **36**, 37-50.

CHIARABBA C., DE GORI P., CHIARALUCE L., BORDONI P., CATTANEO M., DE MARTIN M., FREPOLI A., MICHELINI A., MONACHESI A., MORETTI M., AUGLIERA G.P., D'ALEMA E., FRAPICCINI M., GASSI A., MARZORATI S., DI BARTOLOMEO P., GENTILE S., GOVONI A., LOVISA L., ROMANELLI M., FERRETTI G., PASTA M., SPALLAROSSA D. & ZUNINO E. (2005b) - *Mainshocks and aftershocks of the 2002 Molise seismic sequence, southern Italy.* J. Seism., **9**, 487-494.

CHIARABBA C., JOVANE L. & DI STEFANO R. (2005a) - *A new view of Italian seismicity using 20 years of instrumental recordings.* Tectonophysics, **395**, 251-268.

CINQUE A., ASCIONE A. & CAIAZZO C. (2000) - *Distribuzione spazio-temporale e caratterizzazione della fagliazione quaternaria in Appennino meridionale.* In: Galdini F., Meletti C. & Rebez A. (eds.), Le ricerche del GNDT nel campo della pericolosita sismica (1996 e 1999). CNR-GNDT, Roma, 107-136.

CINTI F., CUCCI L., PANTOSTI D., D'ADDEZIO G. & MEGHRAOUI M. (1997) - *A major seismogenetic fault in a silent area: the Castrovillari fault (southern Apennines, Italy).* Geoph. J. Int., **130**, 595-605.

COCCO M., CHIARABBA C., DI BONA M., SELVAGGI G., MARGHERITI L., FREPOLI A., LUCENTE F.P., BASILI A., JONGMANS D. & CAMPILLO M. (1999) - *The April 1996 Irpinia seismic sequence: evidence for fault interaction.* J. Seism., **3**, 105-117.

CUCCI L., PONDRELL S., FREPOLI A., MARIUCCI M.T. & MORO M. (2004) - *Local pattern of stress field and seismogenic sources in the Pergola-Melandro basin and the Agri valley (Southern Italy).* Geoph. J. Int., **156**, 575-583.

D'AGOSTINO N., MANTENUTO S., D'ANASTASIO E., AVALLONE A., BARCHI M., COLLETTINI C., RADICIONI F., STOPPINI A. & FASTELLINI G. (2008) - *Contemporary crustal extension in the Umbria-Marche Apennines from regional CGPS networks and comparison between geodetic and seismic deformation.* Tectonophysics, **476**, 3-12. doi: 10.1016/j.tecto.2008.09.033.

DEL GAUDIO V., PIERRI P., FREPOLI A., CALCAGNILE G., VENISTI N. & CIMINI G.B. (2007) - *A critical revision of the seismicity of Northern Apulia (Adriatic microplate-Southern Italy) and implica-*

tions for the identification of seismogenic structures. Tectonophysics, **436**, 9-35.

DEVOTI R., RIGUZZI F., CUFFARO M. & DOGLIONI C. (2008) - *New GPS constraints on the kinematics of the Apennines subduction.* Earth Planet. Sci. Lett., **273**, 163-174. doi: 10.1016/j.epsl.2008.06.031.

DI BUCCI D. & MAZZOLI S. (2003) - *The October-November 2002 Molise seismic sequence (southern Italy): an expression of Adria intraplate deformation.* J. Geol. Soc. London, **160**, 503-506.

DI BUCCI D., BURRATO P., VANNOLI P. & VALENSISE G. (2010) - *Tectonic evidence for the ongoing Africa-Eurasia convergence in Central Mediterranean foreland areas: a journey among long-lived shear zones, large earthquakes, and elusive fault motions.* J. Geoph. Res., **15**, B12404. doi: 10.1029/2009JB00648.

DI BUCCI D., RAVAGLIA A., SENO S., TOSCANI G., FRACASSI U. & VALENSISE G. (2006) - *Seismotectonics of the southern Apennines and Adriatic foreland: Insights on active regional E-W shear zones from analogue modelling.* Tectonics, **25**. doi: 10.1029/2005TC001898.

DI BUCCI, D. RAVAGLIA, A. SENO, S. TOSCANI, G. FRACASSI, U. & VALENSISE G. (2007) - *Modes of fault reactivation from analogue modeling experiments: Implications for the seismotectonics of the Southern Adriatic foreland (Italy).* Quaternary International, **171-172**, 2-13.

DI LUCCIO F., FUKUYAMA E. & PINO N.A. (2005a) - *The 2002 Molise earthquake sequence: what can we learn about the tectonics of southern Italy?* Tectonophysics, **405**, 141-154.

DI LUCCIO F., PISCINI A., PINO N.A. & VENTURA G. (2005b) - *Reactivation of deep faults beneath Southern Apennines: evidence from the 1990-1991 Potenza seismic sequences.* Terra Nova, **17**, 586-590. doi: 10.1111/j.1365-3121.2005.00653.x.

EKSTROM G. (1994) - *Teleseismic analysis of the 1990 and 1991 earthquakes near Potenza.* Annali di Geofisica, **37**, 1591-1599.

FAURE WALKER J., ROBERTS G.P., SAMMONDS P. & COWIE P. (2010) - *Comparison of earthquake strains over 10^2 and 10^4 year timescales: insights into variability in the seismic cycle in the central Apennines, Italy.* J. Geoph. Res., **115**, B10418. doi: 10.1029/2009JB006462.

FERRANTI L., OLDOW J.S., D'ARGENIO B., CATALANO R., LEWIS D., MARSELLA E., MASCHIO L., PAPPONE G., PEPE F. & SULLI A. (2008) - *Active Deformation In Southern Italy, Sicily And Southern Sardinia From Gps Velocities Of The Peri-Tyrrhenian Geodetic Array (Ptga).* Boll. Soc. Geol. It. (*Italian Journal of Geosciences*), **127**, 299-316.

FINETTI I. (1982) - *Structure, stratigraphy and evolution of Central Mediterranean Sea.* Boll. Geof. Teor. Appl., **24**, 247-312.

FRACASSI U. & VALENSISE G. (2007) - *Unveiling the Sources of the Catastrophic 1456 Multiple Earthquake: Hints to an Unexplored Tectonic Mechanism in Southern Italy.* Bulletin of the Seismological Society of America, **97**, 725-748.

FREPOLI A. & AMATO A. (2000) - *Fault Plane Solutions of Crustal Earthquakes in Southern Italy (1988-1995): seismotectonic Implications.* Annali di Geofisica, **43**, 437-467.

FREPOLI A., MAGGI C., CIMINI G.B., MARCHETTI A. & CHIAPPINI M. (2011) - *Seismotectonic of Southern Apennines from recent passive seismic experiments.* J. Geodyn., **51**, 110-124.

GALLI P., GALADINI F. & PANTOSTI D. (2008) - *Twenty years of paleoseismology in Italy.* Earth Sci. Rev. doi: 10.1016/j.earseirev.2008.01.001.

GASPERINI P., VANNUCCI G., TRIPONE D. & BOSCHI E. (2010) - *The Location and Sizing of Historical Earthquakes Using the Attenuation of Macroseismic Intensity with Distance.* Bulletin of the Seismological Society of America, **100**, 2035-2066. doi: 10.1785/0120090330.

GASPERINI P., BERNARDINI F., VALENSISE G. & BOSCHI E. (1999) - *Defining seismogenic sources from historical earthquake felt reports.* Bulletin of the Seismological Society of America, **89**, 94-110.

GUIDOBONI E. & COMASTRI A. (2005) - *Catalogue of Earthquakes and Tsunamis in the Mediterranean Area from the 11th to the 15th Century.* Istituto Nazionale di Geofisica e Vulcanologia-Storia Geofisica Ambiente, Bologna, 1037 pp.

GUIDOBONI E. & FERRARI G. (2004) - *Integrazione di ricerca di archeologia e storia territoriale riguardante il terremoto del 1456 e l'area molisanocampana relativamente ai terremoti prima del Mille.* RPT 255/03, Storia Geofisica Ambiente, Bologna, 139 pp.

GUTENBERG B. & RICHTER C.F. (1944) - *Frequency of earthquakes in California.* Bullettin of seismological Society of America, **34**, 185-188.

JENNY S., GOES S., GIARDINI D. & KAHLE H.G. (2006) - *Seismic potential of Southern Italy.* Tectonophysics, **415**, 81-101.

KANAMORI H. & ANDERSON D. (1975) - *Theoretical basis of empirical relations in seismology.* Bulletin of the Seismological Society of America, **65**, 1073-1095.

KOVESLIGETHY R. (1907) - *Seismicher Starkegrad und Intensitat der Beben.* Gerlands Beitr. z. Geophysik, **8**, 363-366.

LATORRE D., AMATO A. & CHIARABBA C. (2010) - *High-resolution seismic imaging of the Mw 5.7, 2002 Molise, southern Italy, earthquake area: Evidence of deep fault reactivation.* Tectonics, **29**, TC4014. doi: 10.1029/2009TC002595.

MAGRI G. & MOLIN D. (1979) - *Attività macrosismica in Basilicata, Campania e Puglia dal 1847 al 1861.* CNEN, RT/AMB (79) 5, pp. 104.

MASCHIO L., FERRANTI L. & BURRATO P. (2005) - *Active extension in Val d'Agri area, Southern Apennines, Italy: implications for the geometry of the seismogenic belt.* Geoph. J. Int., **162**, 591-609. doi: 10.1111/j.1365-246X.2005.02597.x.

MAZZOTTI S. & ADAMS J. (2005) - *Rates and uncertainties on seismic moment and deformation in eastern Canada.* J. Geoph. Res., **110** (B9), B09301.

MELETTI C., PATACCA E., SCANDONE P. & FIGLIUOLO B. (1988) - *Il Terremoto del 1456 e la sua interpretazione nel quadro sismotettonico dell'Appennino Meridionale*. In Il Terremoto del 1456, B. Figliuolo (Editor), Osservatorio Vesuviano, Storia e Scienze della Terra, 71-108 (I) and 35-163 (II).

MENARDI NOGUERA A. & REA G. (2000) - *Deep structure of the Campanian-Lucanian arc (Southern Apennine Italy).* Tectonophysics, **324**, 239-265.

MILANO G., DI GIOVANBATTISTA R. & VENTURA G. (2005) - *Seismic constraints on the present-day kinematics of the Gargano foreland, Italy, at the transition zone between the southern and northern Apennine belts.* Geoph. Res. Let. doi: 10.1029/2005GL024604.

MOLNAR P. (1979) - *Earthquake recurrence intervals and plate tectonics*, Bulletin of the Seismological Society of America, **69**, 115-133.

MONTONE P., MARIUCCI M.T., PONDRELLI S. & AMATO A. (2004) - *An improved stress map for Italy and surrounding regions (central Mediterranean).* J. Geoph. Rese., **109**. doi: 10.1029/2003JB002703.

NICOL A., WALSH J., BERRYMAN K. & VILLAMOR P. (2006) - *Interdependence of fault displacement rates and paleoearthquakes in an active rift.* Geology, **34**, 865-868

PACE B., PERUZZA L., LAVECCHIA G. & BONCIO P. (2006) - *Layered Seismogenic Source Model and Probabilistic Seismic-Hazard Analyses in Central Italy.* Bulletin of the Seismological Society of America, **96**, 107-132.

PANTOSTI D. & VALENSISE G. (1990) - *Faulting mechanism and complexity of the 23 November, 1980, Campania-Lucania earthquake inferred form surface observations.* Journal of Geophysical Research, **95** (B10), 15, 319-15,341.

PANTOSTI D., D'ADDEZIO G. & CINTI FR. (1993) - *Paleoseismological evidence of repeated large earthquakes along the 1980 Irpinia earthquake fault.* Annali di Geofisica, **36**, 321-330.

PAPANIKOLAOU I.D. & ROBERTS G.P. (2007) - *Geometry, kinematics and deformation rates along the active normal fault system in the southern Apennines: Implications for fault growth.* J. Struct. Geol., **29**, 166-188.

PAPANIKOLAOU I.D., ROBERTS G.P. & MICHETTI A.M. (2005) - *Fault scarps and deformation rates in Lazio-Abruzzo, Central Italy: Comparison between geological fault slip-rate and GPS data.* Tectonophysics, **408**, 147-176.

PAPAZACHOS C.B. & KIRATZI A. (1992) - *A formulation for reliable estimation of active crustal deformation and its application to central Greece.* Geoph. J. Int., **111**, 424-432.

PERUZZA L., PACE B. & VISINI F. (2011) - *Fault-Based Earthquake Rupture Forecast in Central Italy: Remarks after the L'Aquila Mw 6.3 Event.* Bulletin of the Seismological Society of America, **101** (1), 404-412. doi: 10.1785/0120090276.

PICCARDI L. (1998) - *Cinematica attuale, comportamento sismico e sismologia storica della faglia di Monte Sant'Angelo (Gargano, Italia): la possibile rottura superficiale del "leggendario" terremoto del 493 d.C.* Geogr. Fis. Dinam. Quat., **21**, 155-166.

PICCARDI L. (2005) - *Paleoseismic evidence of legendary earthquakes: The apparition of Archangel Michael at Monte Sant'Angelo (Italy).* Tectonophysics, **408**, 113 -128.

Pino N.A., Palombo B., Ventura G., Perniola B. & Ferrari G. (2008) - *Waveform modeling of historical seismograms of the 1930 Irpinia earthquake provides insight on 'blind' faulting in Southern Apennines (Italy).* J. Geoph. Res. doi: 10.1029/2007JB005211.

Pondrelli S., Salimbeni S., Ekström G., Morelli A., Gasperini P. & Cannuccia G. (2006) - *The Italian CMT dataset from 1977 to the present.* Physics of the Earth and Planetary Interiors, **159**, 286-303.

Porfido S., Esposito E., Vittori E., Tranfaglia, G., Michetti A.M., Blumetti A.M., Ferreli L., Guerrieri L. & Serva L. (2002) - *Aerial distribution of ground effects induced by strong earthquakes in the southern Apennines (Italy).* Surveys in Geophysics, **23**, 529-562.

Savage J.C. & Simpson R.W. (1997) - *Surface strain accumulation and the seismic moment tensor.* Bulletin of the Seismological Society of America, **87**, 1345-1353.

Sawyer R.K. (2001) - *An integrated surface and subsurface interpretation of the stratigraphy, structure and tectonics of the southcentral Apennines of Italy.* Am. Assoc. Petrol. Geol., 2001 Annual Convention Program Abstracts, **10**, 178.

Sella M., Turci C. & Riva A. (1988) - *Sintesi geopetrolifera della Fossa Bradanica (avanfossa della Catena Appenninica meridionale).* Mem. Soc. Geol. It., **41**, 87-107.

Selvaggi G. (1998) - *Spatial distribution of horizontal seismic strain in the Apennines form historical earthquakes.* Annali di Geofisica, **41**, 241-251.

Serpelloni E., Anzidei M., Baldi P., Casula G. & Galvani A. (2005) - *Crustal velocity and strain-rate fields in Italy and surrounding regions: new results from the analysis of permanent and non-permanent GPS networks.* Geoph. J. Int., **161**, 861-880.

Shebalin N.V. (1973) - *Macroseismic data as information on source parameters of large earthquakes.* Physics of the Earth and Planetary Interiors, **6**, 316-323.

Sponheuer W. (1960) - *Methoden zur Herdtiefenbestimmung in der Makroseismik.* Freiburg Forschung-Hoschule, **88**, 117 pp.

Stucchi M., Camassi R., Rovida,A., Locati M., Ercolani E., Meletti C., Migliavacca P., Bernardini F. & Azzaro R. (2007) - *DBMI04, il database delle osservazioni macrosismiche dei terremoti italiani utilizzate per la compilazione del catalogo parametrico CPTI04.* Available from http://emidius.mi.ingv.it/DBMI04/ (last accessed November 2011).

Tondi E., Piccardi L., Cacon S., Kontny B. & Cello G. (2005) - *Structural and time constraints for dextral shear along the seismogenic Mattinata fault (Gargano, southern Italy).* Tectonophysics, **40** (2-3), 134-152.

Turcotte D.L. & Schubert G. (2002) - *Geodynamics.* 456 pp., Cambridge Univ. Press, New York.

Valensise G. & Pantosti D. (2001) - *The investigation of potential earthquake sources in peninsular Italy: A review.* J. Seism., **5**, 287-306.

Vallée M. & Di Luccio F. (2005) - *Source analysis of the 2002 Molise, Southern Italy, twin earthquakes (10/31 and 11/01).* Geoph. Res. Let., **32**, L12309, 1-4.

Westaway R. & Jackson J. (1987) - *The earthquake of 1980 November 23 in Campania-Basilicata (southern Italy).* Geophysical Journal of the Royal Astronomical Society, **90**, 375-443.

Westaway R. (1992) - *Seismic moment summation for historical earthquakes in Italy: tectonic implications.* J. Geoph. Res., **97**, 15437-15464.

Working Group CPTI (2004) - *Catalogo Parametrico dei Terremoti Italiani, version 2004 (CPTI04). INGV.* Bologna. http://emidius.mi.ingv.it/CPTI/ (last accessed November 2011).

Working Group MPS (2004) - *Redazione della mappa di pericolosità sismica prevista dall'Ordinanza PCM del 20 marzo 2003, rapporto conclusivo.* 65 pp., Dip. della Protez. Civ., Ist. Naz. di Geofis. e Vulcanol., Milan, Italy, April.

Manuscript received 11 January 2011; accepted 23 November 2011; published online 27 March 2012; editorial responsability and handling by D. Pantosti.